P-13-40

Impact of gas generation on radionuclide release – comparison between results for new and old data

Luis Moreno, LMQuimica

Ivars Neretnieks, Chemima AB

October 2013

Svensk Kärnbränslehantering AB
Swedish Nuclear Fuel
and Waste Management Co

Box 250, SE-101 24 Stockholm
Phone +46 8 459 84 00

ISSN 1651-4416
SKB P-13-40
ID 1404589

Impact of gas generation on radionuclide release – comparison between results for new and old data

Luis Moreno, LMQuimica

Ivars Neretnieks, Chemima AB

October 2013

Abstract

New data on metal corrosion rates, radionuclide inventory, sorption coefficients, hydraulic data for bentonite and other data have been obtained (Appendices A and B). The new data have an influence on gas generation rates and rates of release of radioactivity. In the present report the impact of the new data on the results presented in “Project SAFE. Gas related processes in SFR” (Moreno et al. 2001) are explored. The objective is to assess the impact on the radionuclide release and to compare with the results using the old data (Moreno et al. 2001) without, at this stage, to redo all the detailed calculations and to repeat all the underlying thinking. Essentially only the non-sorbing radionuclides are addressed since the impact of the gas generation in the repository is by far strongest for these radionuclides. The gas generation occurs at early times and the sorbing nuclides then have not had time to penetrate the barriers to any appreciable extent.

The new data lead to changes in a large number of processes and parameters. The most important changes in the new calculations, compared with those in the old report, are the new waste inventory, in particular the amounts of metals (steel and aluminium/zinc) and the corrosion rate for steel and iron, which is reduced from 1 to 0.05 μm/year. A list with some of the additional changes is shown below.

- **New gas generation rate for bitumen-stabilized resins**. The gas generation from bitumen-stabilized resins was neglected in the previous calculations and is addressed. Gas formation rates and volumes are now included.
- **New lower flowrates through the repository tunnels and encapsulations**. This decreases the release of radionuclides into the Far-Field.
- **Changes in sorption coefficients**. No large impact is expected since gas related processes primarily impact the release of non-sorbing radionuclides. This is not treated in detail as it is outside the scope of this report.
- **Changes in waste inventory**. The new inventory is very different from the old inventory, Moreno et al. (2001) and the nuclide release is affected.
- **Changes in other parameter data.** (Diffusivity, porosity, density). These data do not influence the release caused by gas formation.

Sammanfattning

Nya uppgifter om metallkorrosionshastigheter, radionuklidinventarium, sorptionskoefficienter, hydrauliska data för bentonit och andra data har tagits fram (Appendixar A och B). De nya data påverkar gasbildningshastighet och utsläppsrater av radioaktivitet. I föreliggande rapport beskrivs inverkan av de nya uppgifterna på de resultat som presenterades i "Project SAFE. Gas related processes in SFR" (Moreno et al. 2001). Syftet med rapporten är att bedöma effekterna på radionuklidutsläpp och jämföra dem med resultaten från de gamla uppgifterna (Moreno et al. 2001) utan att i detta skede, göra om alla detaljerade beräkningar och att upprepa allt det bakomliggande tänkandet. I huvudsak behandlas bara de icke-sorberande radionuklidera eftersom effekterna av gasbildning i förvaret har störst inverkan på dessa radionuklider. Gasutveckling sker tidigt och sorberande nuklider har då inte har haft tid att frigöras från avfallet i någon nämnvärd utsträckning.

De nya data leder till förändringar i ett stort antal processer och parametrar. De viktigaste ändringarna i de nya beräkningarna jämfört med de gamla är avfallsinventariet, särskilt metallmängder (Stål och aluminium/zink) och korrosionshastigheten för stål och järn vilken reducerats från 1 till 0.05 µm/år. Nedan beskrivs några av de viktigaste förändringarna.

- **Ny gasbildningshastighet för bitumenstabiliserade jonbytarmassor.** Gasutveckling från bitumen-stabiliserade jonbytarmassor behandlades inte i de tidigare beräkningarna men ingår nu. Gasvolymer och gasutvecklingshastigheter, och hur dessa påverkar utsläpp av nuklider uppskattas.
- **Nya lägre flöden genom tunnlar och förvarsdelar.** Detta minskar utsläpp av radionuklider till fjärrområdet.
- **Förändringar i sorptionskoefficienter.** Ingen stor påverkan förväntas eftersom gas relaterade processer främst påverkar frisättningen av icke-sorberande radionuklider. Detta behandlas inte i detalj eftersom det är utanför ramen för denna rapport.
- **Förändringar i avfallsinventariet**. Det nya inventariet är väsentligt annorlunda än den tidigare, Moreno et al. (2001) och det påverkar utsläppet.
- **Förändringar i andra parameterdata. (**Diffusivitet, porositet, densitet). Dessa uppgifter påverkar inte märkbart utsläpp orsakade av gasbildning.

Contents

1 Background and general aspects

The gas production causes contaminated water to be expelled into the buffer or gravel/sand around the concrete structure and finally into fractures in the rock surrounding the repository. The amount of water expelled depends on the increased pressure in the vaults caused by the gas generation. For concrete under water-saturated conditions the gas cannot escape unless it reaches a sufficient pressure to overcome the capillary forces in the media surrounding the waste. This may be the buffer surrounding the Silo or fine fractures in the concrete walls of the different concrete constructions. In most cases it is assumed that the overpressure that builds up is on the order of 15 to 50 kPa. This is equivalent to 1.5 to 5 m water head. These assumptions are identical to those used in the previous modelling, Moreno et al. (2001). The head difference generated by the overpressure drives the water flow through the concrete constructions and buffer. A much lower head will not expel as much water and activity release to water in the fractured rock will be primarily by diffusion. At higher head differences the water expulsion will be faster and the volume of free water that can be expelled will escape in a shorter time. Early expulsion of water is beneficial because it takes time for the free water in the different repository parts to be contaminated. Both effects are considered in this report. The analysis is based on the above-described processes.

Several assumptions and considerations are made in the calculations and the most important are listed below:

- Hydrogen production by corrosion takes place in many different locations and starts at different times. Water will be saturated locally and bubbles will form starting to expel water. The solubility of hydrogen is very low and practically all hydrogen will form gas. Escape by diffusion of the dissolved hydrogen away from the repository is negligible compared to the rates of production.
- Due to the relatively short time required to re-saturate the repository after closure it is assumed that all pores and voids in the repository become completely water-filled when the repository is sealed. Any air present in the concrete structure when the gas generation starts will reduce the volume of water expelled.
- Gas cannot flow through fully water-saturated concrete. Therefore a certain water volume has to be expelled from the concrete to create paths for the gas flow. If the gas generation rate is increased pressure will rise and more water will be purged to open more pores. It is assumed that 2% of the water in the concrete (porous and construction concretes) is expelled to establish flow paths for the gas.
- Water may also be expelled from the encapsulation to equilibrate the inner overpressure with the pressure existing outside of the structure. When the pressures have been equilibrated no more water will be expelled.
- The gas generation in the first years is very high, caused mainly by the anaerobic corrosion of aluminium and zinc, which are depleted in a few years. After the aluminium and zinc have corroded the gas generation is determined mainly by the corrosion of iron.
- In general, water availability is not a limiting factor for the gas generation. For each Nm^3 of gas generated, only about one litre of water is required. Water availability may be a limiting factor only during the re-saturation of the repository.
- Very high pressures are needed to expel water from the concrete and allow the gas to flow. The concrete structures in SFR are not designed for these high pressures and they will be damaged if gas cannot escape from the encapsulation.
- If the concrete has small fractures gas flow may be established through these fractures at a lower pressure. In Moreno et al. (2001) an illustrative example of the opening pressure was defined. For fractures with apertures of 10 μm the gas pressure needed to overcome the capillary pressure and flow is 15 kPa. A large number of such fractures is assumed to be present. However, in the silo, gas cannot escape through the outer-wall due to the low hydraulic conductivity of the bentonite around the silo.

- The overpressure needed to overcome the capillary forces in the sand/bentonite above the Silo is 50 kPa.
- The overpressure lowers the water level in the repository part so that for an overpressure of 15 kPa or 50 kPa sinks by 1.5 or 5 m respectively when steady state conditions are reached. At higher overpressures all free water can be expelled from the Silo and 1BMA.
- The calculations are, in general, done in three steps. In the first step, water is expelled to allow the gas flow. The duration of this step is mostly less than one year. In the second step water is expelled from the encapsulation to equilibrate the pressure in its interior. The duration of this step depends on the hydraulic conductivity of the barriers and the gas generation rate. When water expulsion stops a fraction of or all free water has been expelled. After that no more water is expelled from the encapsulation. The calculations are carried out to 1,000 years.

In Chapters 3 to 5 the expelled water volumes and their contamination is calculated for the different repository parts. This water will reside in the backfill materials where such exist and in the empty parts in the tunnels. In some extreme cases a large water volume is expelled into the surrounding rock. In Chapter 6 the fate of the expelled water and its contamination is calculated and compared with the previous modelling.

2 Aims and scope

The aim of this report is to assess how different gas generation rates and hydraulic properties of concrete and buffer influence the rate of release of nuclides from the different parts of the SFR-repository. Only the non-sorbing radionuclides are addressed since the impact of the gas generation in the repository is by far strongest for these radionuclides. The impact of changes in inventory, diffusivity, porosity, density and sorption coefficients is outside the scope of the report. However, when it is obvious that these entities may have an impact it is mentioned.

It is assumed that the reader is familiar with the earlier report, Moreno et al. (2001), and the mechanisms and processes upon which the calculations of gas and water release are based. Details of the models and modelling can be found in Project SAFE (Lindgren et al. 2001). Therefore only a brief description of how the release data are modified for the same cases and scenarios that are described in that report is given. It is therefore recommended that the reader revisits the earlier report.

The report addresses only dissolved radionuclides in the liquid phase.

3 Gas generation in the Silo

- In the first step, when water is expelled to allow the gas flow, it is expected that the steel packages (moulds and drums) are intact and no contamination escapes through the steel wall. After that the steel packages are corroded and radionuclides can escape through the walls.
- Activity from the concrete moulds is only transported by diffusion through the concrete walls. The time to reach a significant concentration in the porous concrete is expected to be of the order of a few years for non-sorbing species. But even for weakly sorbing radionuclides this time is expected to be much longer.
- Due to the presence of waste containing aluminium and zinc it is expected that the corrosion of metals and gas generation starts very early and that during the first year enough gas is generated to expel the water from the porous concrete surrounding the moulds and drums to create flow paths to allow the gas flow.
- For the bitumen-conditioned waste radionuclides in the bitumen mixture are not available for dissolution. These radionuclides are dissolved only when the bitumen matrix degrades. This takes place over a 100-year time scale (Pettersson and Elert 2001).
- Data for gas generation rate and total gas volumes are shown in Tables 3-1 and 3-2 for the new data (see Appendix A) as well as those in Moreno et al. (2001) called old data. It is seen that the data can be quite different for individual items but the overall rates and total volumes change much less.
- In these calculations we have included the possible gas generation from ion-exchange resins in bitumen. The gas generation rate from bitumen is uncertain and the assumed values are conservative. Therefore, these values are written in parentheses in the tables.

Table 3-1. Gas generation rates and total gas volumes due to corrosion for the Silo.

	New data. Initial gas generation rate, (Nm^3/y)	Old data. Initial gas generation rate, (Nm^3/y)	New data. Total gas volumes, (Nm^3)	Old data. Total gas volumes, (Nm^3)
Packaging	22	550	1,107,305	1,200,000
Reinforcement	13	204	755,012	610,000
Structures	4	82	241,703	240,000
Waste				
Steel (waste)	10	8	649,029	20,000
Al/Zn (waste)	4,628	1,080	11,427	2,700
TOTAL	**4,677**	**1,920**	**2,764,476**	**2,100,000**

Table 3-2. Gas generation rates and total gas volumes from corrosion and degradation for the Silo.

	New data. Initial gas generation rate, (Nm^3/y)	Old data. Initial gas generation rate, (Nm^3/y)	New data. Total gas volumes, (Nm^3)	Old data. Total gas volumes, (Nm^3)
Corrosion				
Steel	49	840	2,753,049	2,100,000
Aluminium/Zinc	4,628	1,100	11,427	2,700
Microbial				
Cellulose + org	55	21	27,189	18,700
(Resins + bitumen)	89	100	1,329,038	1,500,000
TOTAL	**4,821**	**1,961**	**2,791,665**	**2,120,000**
No Al/Zn	**193**	**861**		

3.1 Silo calculation cases

Several cases were addressed for the Silo in Moreno et al. (2001). The impact on the release is estimated using the new gas generation data applied to the same cases as in that report.

- Case B1. Gas escapes through the evacuation pipes in the concrete lid. Two situations are distinguished; concrete hydraulic conductivity of $8 \cdot 10^{-12}$ m/s (Case B1a) and $8 \cdot 10^{-10}$ m/s (Case B1b).
- Case ID1. Initial fracture in the bottom of the Silo and gas escape through the evacuation pipes in the concrete lid. Hydraulic conductivity of the concrete is of less importance since water escapes through the fracture.
- Case ID2. Initial fracture in the bottom and no evacuation pipes in the concrete lid. Hydraulic conductivity of the concrete is of less importance since water escapes through the fracture.
- Case E1. Concrete lid without evacuation pipes. Two situations are calculated; concrete hydraulic conductivity of $8 \cdot 10^{-12}$ m/s (Case E1a) and $8 \cdot 10^{-10}$ m/s (Case E1b).

3.2 Case B1. Gas escape through evacuation pipes in the concrete lid

Gas escapes through the evacuation pipes in the concrete lid. Water expelled to allow the gas flow also escapes through the evacuation pipes on the top. Water to equilibrate the overpressure in the Silo escapes through the Silo walls and bottom as shown schematically in Figure 3-1. In Case B1a, most water escapes through the vertical wall, in Case B1b, most water escapes through the bottom. It is assumed that the silo top is located 50 m below the sea level.

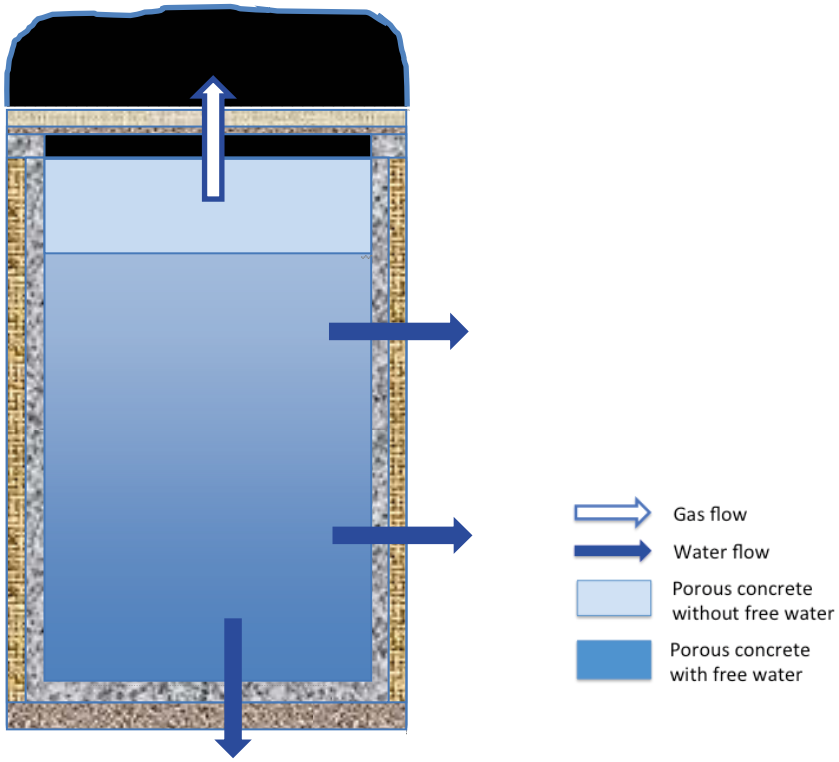

Figure 3-1. *Gas and water flow escaping from the Silo for the Case B1 (Not at scale).*

3.2.1 Step 1. Gas generation starts and water is expelled from Silo through evacuation pipes

- The water expelled from the Silo during the pressure build up period may escape through the evacuation pipes or through the Silo walls. However, it is assumed that all this water volume is expelled through the evacuation pipes in less than one year.
- The water expelled (72.5 m^3) through the gas evacuation pipes enters the sand layer and sand-bentonite sealing on top of the Silo. The water volume in these layers is about 150 m^3, therefore the volume of water expelled stays within these layers. Subsequent radionuclide release will be mainly by diffusion into the sand/gravel on the top of Silo.
- The moulds and drums have a free volume inside of them that will become water filled after sealing of the Silo. For the drums and moulds made of steel it is assumed that the walls are intact when the gas generation starts and the gas produced escapes through the top of the containers. For the concrete moulds it is also expected that the gas escapes through the top. If the gas cannot escape through the top fractures could be created in the concrete walls and a part of the free water could be expelled.

Consequences

- Applying the new gas generation data, it is found that the impact on radionuclide release is very small. The concentration of radionuclides in the pore-water in the grout is low at early times. Therefore, the activity release during the initial step, using the new data, will be somewhat lower, since the new gas generation rate is higher and more water will be expelled at shorter times. However, in the calculations we have kept the assumptions that the water volume of 72.5 m^3 is expelled in one year.
- The values used for the hydraulic conductivity of bentonite and concrete have no impact on the release in this step, since it is conservatively assumed that all the water is expelled through the evacuation pipes.

3.2.2 Step 2. Water is expelled to equilibrate the pressure in the Silo

- Water is expelled through the outer wall and the bottom-wall to equilibrate the pressure inside the Silo with the pressure in the surroundings. For an overpressure of 50 kPa, the water level is lowered by 5 m and 200 m^3 of water are expelled. For comparison, the total volume of free water is about 2,000 m^3.
- If the pressure required to expel the gas through the sand/bentonite layer is higher the volume of water expelled to equilibrate the overpressure in the silo will be increased. For an overpressure of 100 kPa, the volume of water to be expelled will be 400 m^3 for the cases B1 and ID1. The other cases are not affected since no gas escapes through the sand/bentonite. Therefore the release of contaminants will be increased by a factor 2, since it is expected that the times for the water expulsion will be almost the same.
- When equilibrium is reached no more water is expelled from the Silo. Radionuclides are then released by diffusion through the Silo wall and top and bottom-walls.
- Two cases are considered. In the first case the hydraulic conductivity of the concrete is lower ($8 \cdot 10^{-12}$ m/s). The water will be expelled over a longer time through both the bottom-wall and the Silo wall.
- For the other case the hydraulic conductivity of the concrete is $8 \cdot 10^{-10}$ m/s, as may be expected for construction concrete. The water will be expelled during a shorter time mainly through the bottom-wall of the Silo since the sand-bentonite layer at the bottom has a higher hydraulic conductivity than the bentonite around the Silo wall.
- If the water volume expelled is larger than the sorption capacity (pore volume for non-sorbing species) of the concrete walls some contaminated water may flow into the bentonite or sand-bentonite.

- The maximum flowrate with which the water can be expelled from the Silo is the gas generation rate at the existing pressure. When all aluminium and zinc has been consumed (about 2.5 years) the gas generation is 193 Nm^3/year or 35 m^3/year at the pressure in the Silo. This means that water may be expelled from the Silo with a maximum flowrate of 35 m^3/year.
- For Case B1a, with a concrete hydraulic conductivity of $8 \cdot 10^{-12}$ m/s, the time for expulsion of most of the 200 m^3 water is about 100 years. For case B1b with a hydraulic conductivity of $8 \cdot 10^{-10}$ m/s, this time is about 10 years. When the time is shorter less activity is present in the water and the release of activity will be smaller.
- The hydraulic conductivity of the bentonite around the Silo has been modified. Using the new values it is expected that a larger volume of water will be expelled through the bottom-wall. Theses values are shown in Table 3-3 and compared with the old distribution, Moreno et al. (2001). Bentonite barrier is divided is two halves; both with 25 m in high.
- With the new values for hydraulic conductivity for bentonite around the Silo the maximum intrusion of contaminated water is into the bottom-wall for the case with construction concrete with a hydraulic conductivity of $8 \cdot 10^{-10}$ m/s. This water volume is 116 m^3, of which about 24 m^3 flows into the sand/bentonite in the bottom; the remainder is kept in the concrete bottom-wall. The water volume into the sand/bentonite corresponds only to 10% of the pore-water in this layer. For the old values of bentonite hydraulic conductivity the water volume expelled through the bottom is 84 m^3, therefore, no water is expelled into the sand/bentonite in the bottom. The water is kept in the concrete bottom-wall. In both cases, the more contaminated water is located close to the inner part of the bottom-wall. The subsequent early release by diffusion is only slightly increased.

Consequences

- The water volume expelled to equilibrate the water pressure in the Silo is not influenced by the new gas generation rates in both cases (Case B1a and Case B1b). The flowrate of contaminated water expelled from the Silo is only controlled by the hydraulic conductivity of the barriers, regardless the value of the gas generation rate. The only condition is that the gas generation rate at the respective pressure has to be higher than the water flowrate.
- The new hydraulic conductivities for the bentonite around the silo increase the volume of water potentially contaminated expelled into the bottom-wall for the case with construction concrete with a hydraulic conductivity of $8 \cdot 10^{-10}$ m/s. The effect will be small since the diffusion distance in the sand/bentonite is large enough. At the same time the concentration in the porous concrete continues to increase, which also diffuses through the bottom-wall dominating the release of activity through the bottom with time.

Table 3-3. Distribution of the expelled water between the different Silo walls, in volume fraction. In parenthesis volume of water expelled m^3

Wall	New data	Old data, Moreno et al. (2001)	Volume difference, m^3. [Fraction water in wall]
Good concrete, $K=8 \cdot 10^{-12}$ m/s			
Silo wall, upper part	0.57 (114)	0.72 (144)	–30 [0.02]
Silo wall, lower part	0.28 (56)	0.11 (22)	+34 [0.02]
Bottom-wall	0.15 (30)	0.17 (34)	–4 [0.003]
Construction concrete, $K=8 \cdot 10^{-10}$ m/s			
Silo wall, upper part	0.38 (76)	0.57 (114)	–38 [0.02]
Silo wall, lower part	0.04 (8)	0.01 (3)	+3 [0.002]
Bottom-wall	0.58 (116)	0.42 (84)	+32 [0.03]

3.3 Case ID1. Initial fracture in the bottom and gas escape through the evacuation pipes in the concrete lid

Gas escapes through the evacuation pipes in the Silo lid. Water to allow the gas flow in the concrete/cement and to equilibrate the overpressure in the Silo is expelled through the fracture at the bottom. This is schematically shown in Figure 3-2.

The retention capacity of the concrete in the bottom-wall (porosity and sorption) is not used, since the water expelled bypasses the concrete in the bottom through the fracture. The pressure in the Silo is maintained at gas release pressure of 50 kPa and the hydraulic conductivity of the concrete is not important since it is assumed that water does not flow through the concrete walls. The water level is lowered by 5 metres and all the expelled water (272 m^3) flows out through the fracture at the bottom during a time estimated to be 10 years. 72.5 m^3 of water are expelled from the silo to establish flow paths for the gas and 200 m^3 to equilibrate the overpressure in the silo.

- The new hydraulic conductivities for the bentonite around the Silo do not influence the volume of water expelled from the Silo and its flowrate, since these are determined by the overpressure in the Silo (50 kPa) and the gas generation rate.

Consequences

- For the overpressure within the silo of 50 kPa, it is assumed that the 272 m^3 water are expelled in 10 years. Since in both cases (for the old and the new data) the gas generation is sufficient to keep the flow of water escaping from the silo water flow at 27.2 m^3/year, no differences would be observed between both cases.
- The new hydraulic conductivities for the bentonite around the Silo do not influence the volume of water expelled from the Silo and its flowrate.

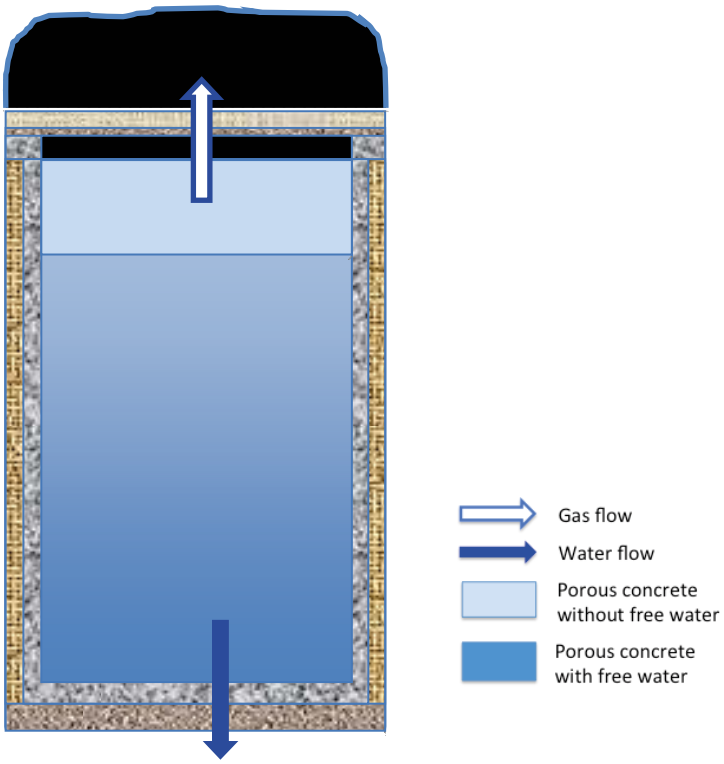

Figure 3-2. *Gas and water flow escaping from the Silo for the Case ID1 (Not at scale).*

3.4 Case ID2. Initial fracture in the concrete bottom and no or clogged evacuation pipes in the lid

Gas cannot escape through the Silo lid and a high pressure is created in the Silo. Therefore, all the free water is expelled from the Silo through the fracture in the bottom. This is schematically shown in Figure 3-3.

- In this case all the free water, 2,070 m^3, is expelled from the Silo as the gas increases in pressure and volume. The hydraulic conductivity of the concrete is $8 \cdot 10^{-12}$ m/s. Since the pressure in the Silo is 10 bar, the volume of gas to be generated necessary to expel all the water is 20,700 Nm^3. If construction concrete with a hydraulic conductivity of $8 \cdot 10^{-10}$ m/s is considered, the gas may flow through micro-fractures in the concrete lid at a lower overpressure and a smaller volume of water is expelled.
- Using the new gas generation data the total gas generation rate is 4,800 Nm^3/year during the first 2.5 years when aluminium and zinc are corroding and a volume of 1,200 m^3 water is expelled from the Silo. The remaining water, 870 m^3 water, is expelled in about 45 years at an average water flowrate of 19.3 m^3/y.
- For the old data, during the 2.5 first years when aluminium and zinc are corroding 490 m^3 of water is expelled. The remaining water, 1,580 m^3, is expelled at a rate of 85 m^3/year during about 19 years.
- The new hydraulic conductivities for the bentonite around the Silo do not influence the flowrate since it is assumed that the water volume is expelled from the Silo through the fracture at the bottom. The water flowrate is determined by the pressure in the Silo, the gas generation rate and the conductivity of the fracture at the bottom.
- Figure 3-4 shows the relative concentration for a non-sorbing species in the grout as a function of time. The term relative concentration was used since the interest was in how the concentration changes with time and not its absolute value. The concentration increases very rapidly in the first 2.5 years and slowly after that. Using these values the amounts of radionuclide released from the Silo for the new and old gas generation data were calculated. It was found that the amount of non-sorbing radionuclide that is released using the new data is 15% smaller than that using the old data. This is because more of the water expulsion occurs earlier when the contamination concentration is lower. This concentration increases very rapidly initially due to release from the steel packages when they are corroded.

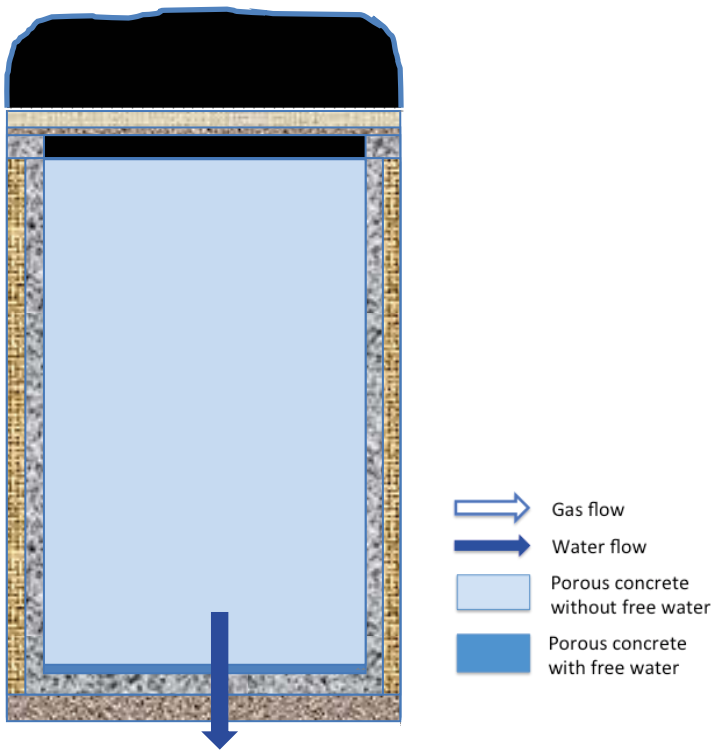

Figure 3-3. *Water flow escaping from the Silo for the Case ID2 (Not at scale).*

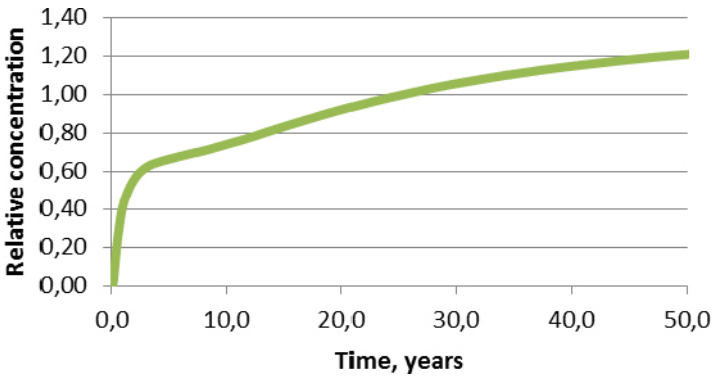

Figure 3-4. *Concentration in the grout as function of time. Absolute values of concentration are not important, only the variation with time is important.*

Consequences

For the new gas generation data the early high gas generation rate implies that a larger volume of water with a lower concentration is expelled from the Silo initially. After that the water is expelled at a low water flowrate with a concentration that increases slowly. The contamination released from the Silo is about 15% smaller using the new gas generation data.

3.5 Case E1. Concrete lid without evacuation pipes

- For Case E1a, with a concrete hydraulic conductivity of $8 \cdot 10^{-12}$ m/s, the pressure in the interior of the Silo is mainly determined by the gas generation rate. Water is expelled from the Silo by the increasing pressure in its interior. The rate is set by the hydraulic conductivity of the barriers. Since the Silo is not designed to withstand high pressure, it is expected that fractures will be created in the Silo walls. However, in the calculations it is pessimistically assumed that all the free water is expelled from the Silo through the walls before the Silo is damaged. Fractures are created later to allow the gas to escape from the Silo.
- For Case E1a, all the 2,070 m^3 free water in the Silo is expelled through the outer and bottom walls. To expel this water volume 20,700 Nm^3 of gas has to be generated. 12,000 Nm^3 is generated during the first 2.5 years and the remainder, 8,700 Nm^3, is generated in 41 years. A large volume of water with low concentration is expelled from the Silo in the first years when aluminium and zinc are corroding. After that water with somewhat higher concentration of radionuclide is slowly released from the Silo. The amount of non-sorbing radionuclides released from the Silo into the Silo walls will be lower for the case using the new gas generation rate since less contaminated water is expelled at earlier times. The release is about 15% lower with the new data. A schematic picture of this case is shown in Figure 3-5.
- For Case E1b, with construction concrete, a moderate pressure is required to create paths for the gas flow. Gas may flow through micro-fractures in the concrete lid. The hydraulic conductivity of the construction concrete is very important in this case. In the calculations, it is as before, assumed that the concrete has a network of micro-fractures with an opening pressure of 15 kPa. This implies that a pressure of 65 kPa (15 kPa through the micro-fractures and 50 kPa through the sand/bentonite layer on the top of the Silo) is needed to allow the gas to escape through the Silo top and sand/bentonite layer. A schematic picture of this case is shown in Figure 3-5.

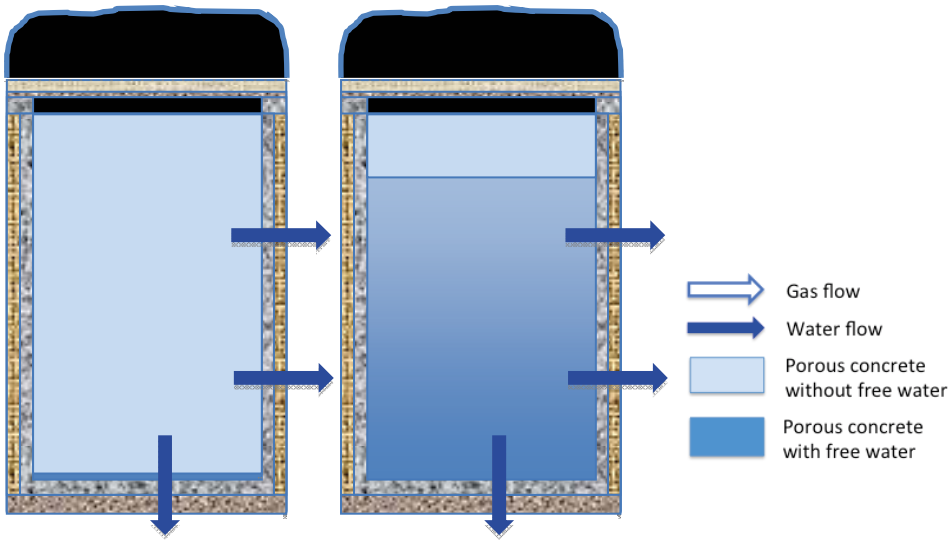

Figure 3-5. *Water flow escaping from the Silo for the Case E1a (left figure) and Case E1b (right figure) (Not at scale).*

Consequences

For Case E1a the amount of non-sorbing radionuclides released from the Silo into the Silo walls will be about 15% lower using the new gas generation rate. For Case E1b the new gas generation rate does not change the radionuclide release from the Silo since in both cases the generated gas is expelled through the lid and the sand/bentonite layer.

3.6 Sensitivity of some assumptions made in release calculations for the Silo

In the models used for calculating the radionuclide release several assumptions were made. One of these assumptions is that the steel moulds or drums in the Silo containing the cement-stabilized waste are intact in the first stage when water is expelled to allow the gas flow in the cement/concrete. Therefore, no contaminated water is expelled from the steel moulds or drums. Contamination may however escape from the concrete moulds by diffusion through the concrete walls. This assumption is based in the fact that the duration of this stage is only one year.

Another assumption used in the calculations is that the waste contains large amount of aluminium and zinc, which are corroded very rapidly. Due to the presence of aluminium and zinc in the waste a large volume of gas is produced in the first 2.5 years. This means that the water is expelled very early from the Silo when the concentration levels are low

Since these assumptions have a large impact on the radionuclide release calculations, a sensitivity analysis is made for both situations. For the first assumption, it is assumed that the walls of the steel moulds and drums are totally corroded from the beginning. The cement-conditioned waste is then in direct contact with the surrounding porous concrete. This implies that the water expelled from the Silo at early times is more contaminated.

For the second assumption, it is assumed that the waste does not contain aluminium and zinc. Therefore, the initial gas generation is strongly reduced. This means that the contaminated water expelled from the Silo, to allow the gas flow and equilibrate the over-pressure, is expelled during a longer time when higher contamination levels are reached. On the other hand, the rate with which the water is expelled is lower, decreasing the contamination rate.

The comparison was made for three cases:

- Case B1a (concrete hydraulic conductivity of 8·10–12 m/s), 72.5 m^3 of water is expelled from the Silo to allow the gas flow in the concrete and cement. The gas escapes through the Silo top creating an overpressure of 50 kPa in the Silo. 200 m^3 of water is expelled to equilibrate the over-pressure. Most the water is expelled through the vertical wall due to its larger surface area compared with the bottom.
- Case B1b is similar to the case B1a, but in this case construction concrete is used with a higher hydraulic conductivity. More water is expelled through the bottom, since the low hydraulic conductivity of the bentonite around the Silo decreases the volume of water expelled through the wall.
- Case ID2 (concrete hydraulic conductivity of $8 \cdot 10^{-12}$ m/s). This is a critical case, with a high release of radionuclide. There is no gas pipe in the Silo lid and there is an initial fracture in the bottom. Therefore, gas cannot escape through the Silo top and 2,070 m^3 water is expelled through the fracture in the bottom.

The comparisons are made for non-sorbing species, since the effect will be less for sorbing species, which escape from the moulds much more slowly because of sorption.

3.6.1 The walls of the steel moulds and drums are totally corroded from the beginning.

The radionuclide release is calculated for two situations: a) (the normal case) the walls of the steel moulds and drums are intact during the first stage when water is expelled to allow the gas flow in the concrete/cement and b) no resistance in walls exists since they are totally corroded.

The radionuclide releases for non-sorbing species are shown in Figures 3-6 to 3-8 for the cases B1a, B1b, and ID2 respectively. For the three cases, the existence of the steel wall in the containers is significant only for times shorter than a few years. Therefore, that the steel moulds and drums were totally corroded from the beginning is only significant for radionuclides with a half-file of a few years.

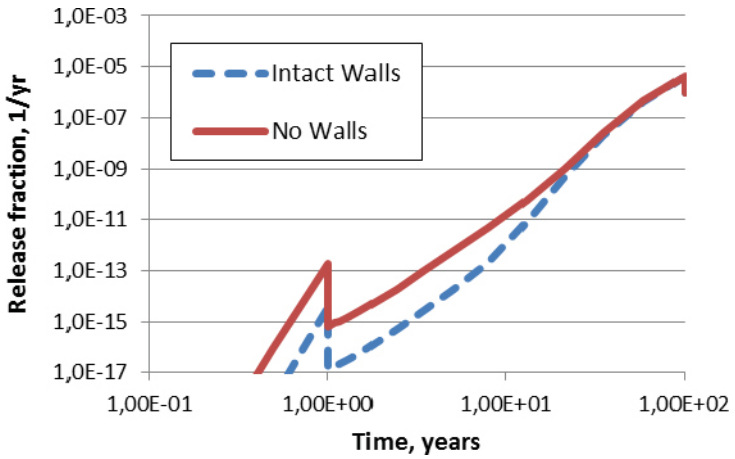

Figure 3-6. *Release fraction for a non-sorbing species for the case B1a for intact and totally corroded steel wall in the moulds and drums.*

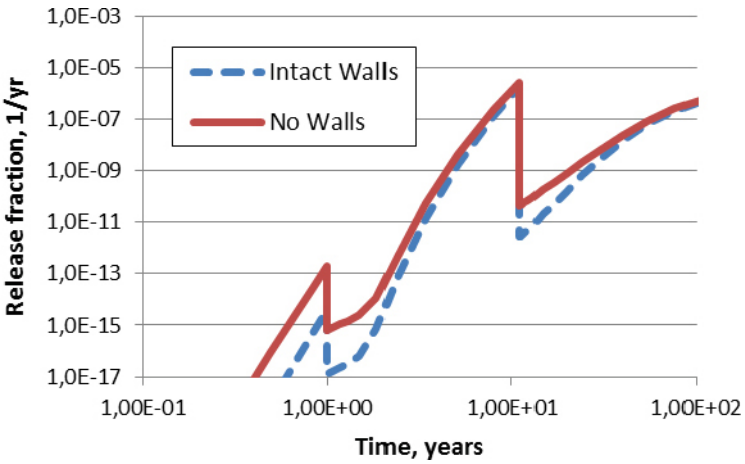

Figure 3-7. *Release fraction for a non-sorbing species for the case B1b for intact and totally corroded steel wall in the moulds and drums.*

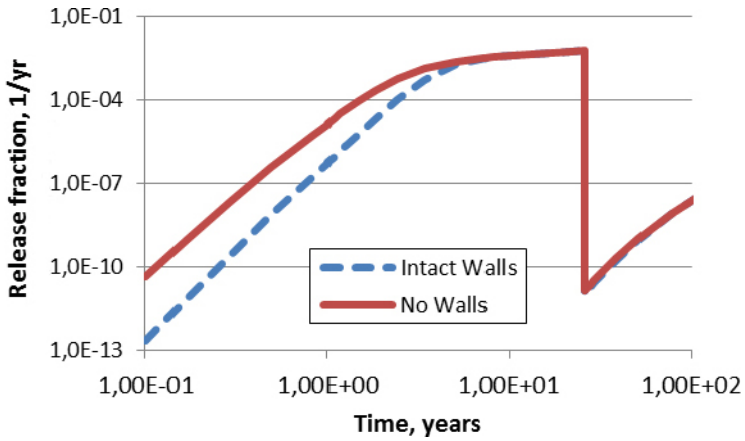

Figure 3-8. *Release fraction for a non-sorbing species for the case ID2 for intact and totally corroded steel wall in the moulds and drums.*

3.6.2 The waste does not contain aluminium/zinc

The radionuclide release is calculated for two situations: a) (the normal case) the waste contains aluminium and zinc and b) the waste does not contain aluminium/zinc. The radionuclide releases for non-sorbing species are shown in Figures 3-9 to 3-11 for cases B1a, B1b, and ID2 respectively.

For both cases, B1a and B1b, the 72.5 m^3 water are expelled in one year to create gas paths in the concrete to allow the gas flow for the case of waste containing aluminium and zinc. For the case of waste without aluminium/zinc this time is assumed to be five years, due to less gas generation.

For case B1a, 200 m^3 of water is expelled to equilibrate the overpressure in the silo. This volume is removed in about 100 years irrespective of if the waste contains aluminium and zinc or not. The results in Figure 3-9 shows that the release rate is higher for waste containing Al and Zn for times less than 2 years. Between 2 and 7 years the release is higher for waste without Al/Zn. After that there are no differences. The differences are caused by the different rates at which the contaminated water is expelled from the silo and the differences in concentration of the expelled water, which increases with time. For case B1b with waste containing aluminium and zinc the release is higher during the first 11 years as shown in Figure 3-10. After about 16 years there are no differences. Between 11 and 16 years the release is larger for the case of waste without aluminium/zinc.

For case ID2 (concrete hydraulic conductivity of $8 \cdot 10^{-12}$ m/s), 2,070 m^3 of contaminated water is expelled from the silo through the fracture at the bottom. For waste containing aluminium and zinc the time is about 25 year, while for waste without aluminium/zinc this water volume is expelled in about 205 years. Figure 3-11 shows that the release is higher for the waste containing aluminium and zinc for times shorter than about 25 years. Between 25 and 300 years, the release is higher for waste without Al/Zn. After that there are no differences.

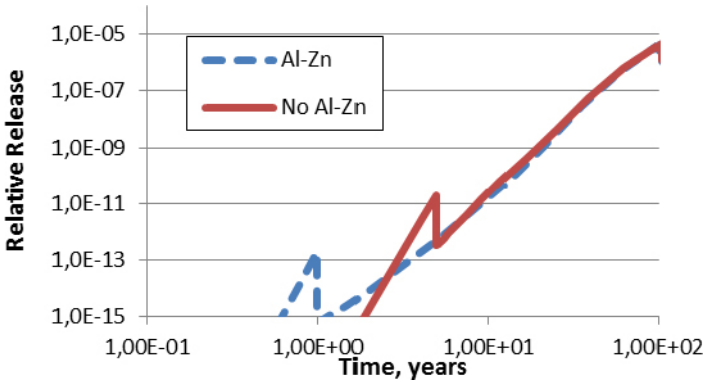

Figure 3-9. *Release fraction for a non-sorbing species for the case B1a for waste with and without aluminium/zinc.*

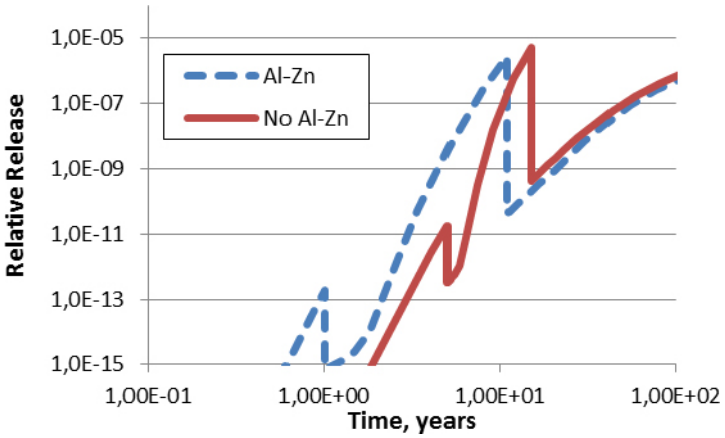

Figure 3-10. *Release fraction for a non-sorbing species for the case B1b for waste with and without aluminium/zinc.*

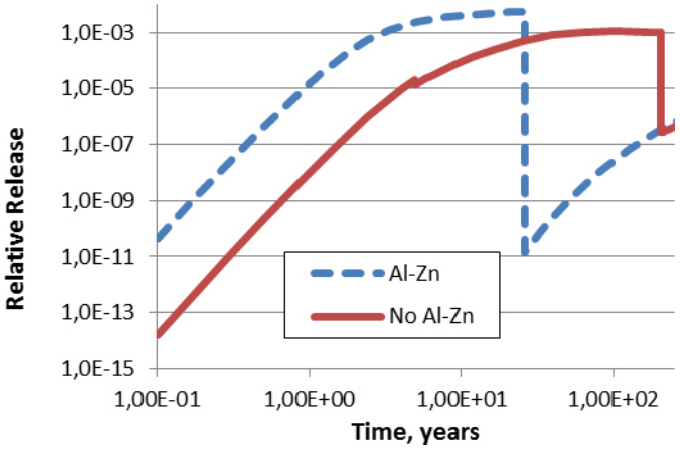

Figure 3-11. *Release fraction for a non-sorbing species for the case ID2 for waste with and without aluminium/zinc.*

4 Gas generation in 1BMA

- The gas reaching the top of the encapsulation is expected to escape through gaps between the concrete lid and the walls of the structure (Case B1).
- The transport of the radionuclides from the waste to the free water occurs mainly by diffusion. A fraction of the activity in the waste packages may be transported with the expelled water.
- Due to the presence of waste containing aluminium and zinc gas generation starts early and during the first year enough gas is generated to expel the water volume to allow the gas flow.
- It is expected that during the first year the steel containers are intact and no contamination escapes from them. After that the steel packages have corroded and lost their barrier function.
- Radionuclides in the bitumen mixture are not available for dissolution. These radionuclides are dissolved only when the bitumen matrix degrades. This takes place over a 100-year time scale (Pettersson and Elert 2001).
- The time to reach a significant concentration in water in the porous concrete around the waste packages is expected to be a few years for non-sorbing species and much longer for sorbing radionuclides.
- During the operational phase, as a vault is filled, a concrete lid is installed over the waste and after that a 5 cm thick concrete layer is cast on top of the lid to prevent water intrusion. At repository closure an additional 0.5 m thick reinforced concrete lid will be cast on top of the compartments. The lid is not hermetically sealed and gas may escape from the encapsulation and negligible overpressure is created in the interior.
- Data for gas generation rates and total gas volumes are shown in Tables 4-1 and 4-2 for the new and old data. It is seen that the data can be quite different for individual items but the overall rates and total volumes change much less.

Table 4-1. Gas generation rates and total gas volumes from corrosion for 1BMA.

	New data. Initial gas generation rate, (Nm^3/y)	Old data. Initial gas generation rate, (Nm^3/y)	New data. Total gas volumes, (Nm^3)	Old data. Total gas volumes, (Nm^3)
Packaging	16	346	701,177	710,000
Reinforcement	10	178	627,376	540,000
Waste	4,448	7,110	307,039	340,000
Steel (Waste)	*6*	*96*	*295,553*	*320,000*
Al/Zn (waste)	*4,442*	*7,020*	*11,486*	*18,000*
Structures	3	54	214,522	210,000
TOTAL	**4,477**	**7,690**	**1,850,114**	**1,800,000**

Table 4-2. Gas generation rates and total gas volumes from corrosion and degradation for 1BMA.

	New data. Initial gas generation rate, (Nm^3/y)	Old data. Initial gas generation rate, (Nm^3/y)	New data. Total gas volumes, (Nm^3)	Old data. Total gas volumes, (Nm^3)
Corrosion				
Steel	35	670	1,838,628	1,800,000
Aluminium/Zinc	4,442	7,000	11,486	16,000
Microbial				
Cellulose + org	275	246	140,053	136,000
(Resins+bitumen)	72	(65)	1,079,234	(980,000)
TOTAL	**4,824**	**7,916**	**3,069,401**	**1,952,000**
No Al/Zn	**382**	**916**	**3,057,915**	**1,936,000**

4.1 1BMA calculation cases

Several cases are calculated for 1BMA:

- Case B1. Gas escapes through gaps between the concrete walls and the lid.
- Case ID. Initial fracture in the concrete bottom and no existing gaps between the walls and lid. Two cases are considered; with concrete hydraulic conductivities of $8 \cdot 10^{-12}$ and $8 \cdot 10^{-10}$ m/s.
- Case E1. No existing gaps between the concrete walls and the lid. Two values are considered for the hydraulic conductivity of the construction concrete, $8 \cdot 10^{-12}$ m/s (Case E1a) and $8 \cdot 10^{-10}$ m/s (Case E1b).
- Case E2. The space between the waste containers is filled with grout.

The modelling of 1BMA is done for a compartment with an average waste composition.

4.2 Case B1. Gas escapes through gaps between the concrete walls and lid

- All the gas escapes through gaps between the lid and the walls in the top of the encapsulation and negligible overpressure is created in the interior of the structure. A schematic picture of the situation is shown in Figure 4-1.
- A volume of 19.3 m^3 water is expelled from 1BMA to allow the gas flow through the concrete/cement during the first year. The walls of the steel containers are intact during the first year but they are not hermetically sealed and water and gas may flow through these openings. The same situation is considered for the concrete moulds, but in this case the water can also penetrate into the waste through the concrete walls.
- In the first years radionuclides migrate into the water surrounding the waste packages by diffusion through the concrete walls of the concrete moulds and by the water expelled from the interior of the waste packages. After that it is assumed that the steel walls have corroded and radionuclides can escape through the walls.

Consequences

Applying the new gas generation data it is found that the impact on radionuclide release is very small since the gas generation rate is very high and the water is expelled in a very short time in both cases.

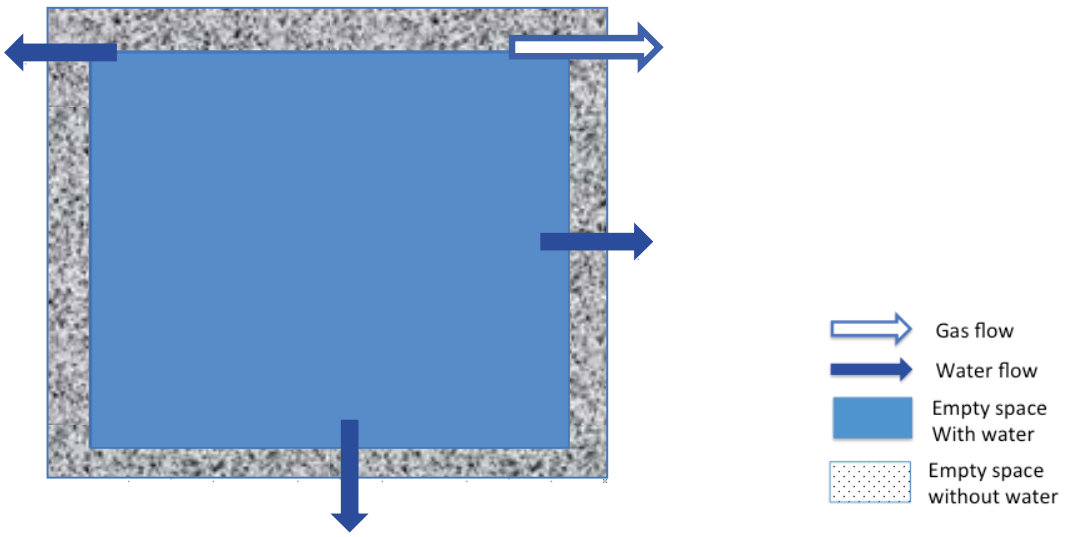

Figure 4-1. *Gas and water flow escaping from 1BMA for Case B1 (Not at scale). Water flows only in the first stage when water is expelled to allow gas flow through concrete/cement.*

4.3 Case ID. Initial fracture in the concrete bottom and no existing gaps between the walls and lid

- If gaps do not exist an overpressure will be created in 1BMA encapsulation. The volume of water expelled through the fracture at the bottom is determined by the hydraulic conductivity of the concrete used in the structure. For construction concrete ($K=8\cdot10^{-10}$ m/s) with small fractures the overpressure needed to overcome capillary forces is, as before, taken to be 15 kPa. A water volume of about 480 m^3 is expelled from 1BMA to equilibrate the overpressure since the water level needs to be lowered by 1.5 m. The total volume of free water that can be expelled from 1BMA is about 3,200 m^3. For high quality concrete ($K=8\cdot10^{-12}$ m/s) gas cannot escape through the concrete walls and all the free water will be expelled through the fracture at the bottom. A schematic picture of the case ID is shown in Figure 4-2.
- For concrete with a hydraulic conductivity of $8\cdot10^{-12}$ m/s all the free water is expelled. For the new gas generation rate, 2,000 m^3 of water is expelled in 2.5 years and the remainder, 1,200 m^3, is expelled in about 19 years. For the old data all the water is expelled in the 2.5 first years.
- For the case with construction concrete the volume of water to be expelled is smaller and takes place very early. It is expected that the new data have negligible impact on the radionuclide release since the initial gas generation rate is very high for both the present data and those in Moreno et al. (2001).

Results and consequences

For the case with concrete with a hydraulic conductivity of $8\cdot10^{-10}$ m/s, it is found that the new gas generation rate has very little impact on the radionuclide release. The water is expelled very early and during a short time since the present generation rate and that in Moreno et al. (2001) are very high and the volume the water expelled is small. After that no more water is expelled.

For the case with concrete with a hydraulic conductivity of $8\cdot10^{-12}$ m/s, the time to expel the water for equilibrating the overpressure in the structure is much longer using the new gas generation rate. This means that the water expelled has enough time to reach a higher concentration. It is expected that the release with the present gas generation data were about a factor two higher than that using the old data. Figure 4-3 shows the evolution of the free water concentration in the encapsulation.

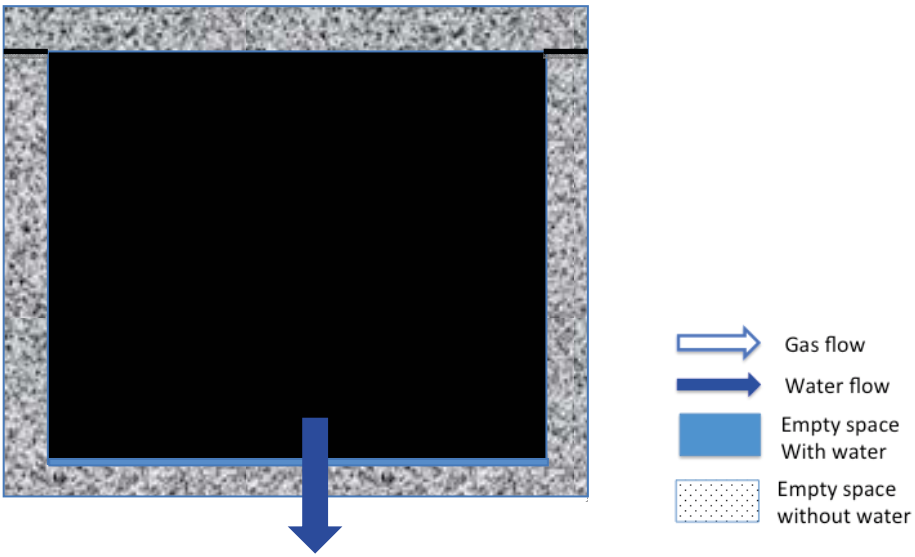

Figure 4-2. *Water flows from 1BMA through a fracture at the bottom, Case ID and good quality concrete ($K= 8\cdot10^{-12}$ m/s) is used for the walls (Not at scale). All the free water is expelled through the fracture in the bottom.*

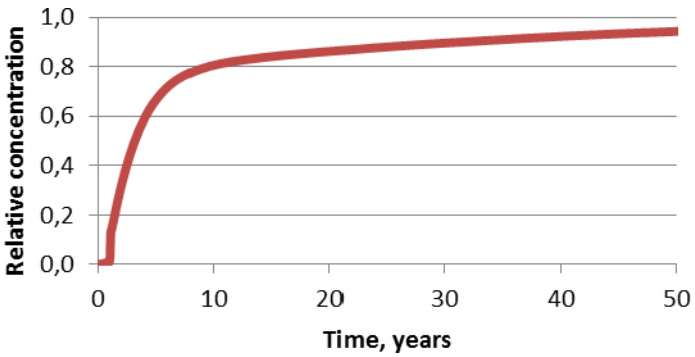

Figure 4-3. *Free water concentration in the encapsulation in 1BMA as a function of time. Absolute values of concentration are not important, only the variation with time is important.*

4.4 Case E1. No existing gaps between concrete walls and lid

- In Case E1a the concrete in the walls are of high quality with a hydraulic conductivity of $8 \cdot 10^{-12}$ m/s. In Case E1b construction concrete in the wall has a hydraulic conductivity of $8 \cdot 10^{-10}$ m/s.
- The Case E1b may correspond to the situation where micro-fractures are created in the concrete walls. For the open pressure 15 kPa the water level is lowered by 1.5 m. The water will be expelled through the walls and the bottom over a period of a few years.
- For Case E1a gas flow through the concrete walls is only possible at very high overpressure. The construction is not designed to support such a high overpressure. Fractures will form in the concrete walls increasing the hydraulic conductivity reaching the Case E1b. However, most probably only a few fractures are formed. The process is as follows: The gas pressure in the container or vault increases until one fracture develops at the weakest point. This fracture can be either large enough to let the gas escape in a rush or let it escape gradually. When it escapes gradually the pressure drops to a level that just balances the gas generation rate and the pressure difference between in- and outside. In this scenario it is assumed that essentially only one escape route is formed.
- Another alternative is that the pressure in the interior of the encapsulation is sufficient to partially lift the concrete lid but maintain a high overpressure in 1BMA. In this case all the free water can be expelled. This is not deemed to be probable since 1BMA is not designed for high pressure and the walls will be damaged and fractures created. If the fractures are created in the upper part of the walls gas can escape from the encapsulation, the pressure decreases and no more water will be expelled. If the fractures occur at the bottom all the water will be expelled through the bottom. This case was discussed in case ID for good concrete.

Results and consequences

For Case E1a, if fractures are created in the upper part of the walls, gas can escape from the encapsulation. The pressure decreases and no more water will be expelled from 1BMA. This was addressed in the Case ID for construction concrete. If fractures form at the bottom, water will be expelled through the bottom and the situation will be similar to that in Case ID for good concrete. For the case with concrete with a hydraulic conductivity of $8 \cdot 10^{-10}$ m/s, the radionuclide release is similar for the new and old data.

4.5 Case E2. No existing gaps between concrete walls and lid and the space between the waste containers filled with grout

- In 1BMA a large volume of water is free in the interior of the encapsulation and can be expelled if the pressure increases. To reduce the volume of free water and increase the sorption capacity it has been proposed that the space between the waste containers should be backfilled with grout.
- The calculations are made only for the case with an initial fracture at the bottom and no gaps between the lid and the walls. For a concrete with a hydraulic conductivity of $8 \cdot 10^{-12}$ m/s. It is expected that all the water is expelled through a fracture assumed to form at the bottom. The addition of backfill grout reduces the volume of free water in 1BMA by 50% to about 1,600 m^3.

Consequences

It is expected that for the old data and new data the radionuclide release will be similar.

4.6 Sensitivity to some assumptions made in release calculations for 1BMA

In the models used for calculating the radionuclide release, it was assumed that the steel moulds or drums in 1BMA are intact in the first stage when water is expelled to allow the gas flow in the cement/concrete. Therefore, no contaminated water is expelled from the steel moulds or drums. Contamination may however escape from the concrete moulds by diffusion through the concrete walls. This is because the duration of this stage is only one year.

Another assumption is that the waste contains large amount of aluminium and zinc, which are corroded very rapidly. Due to the presence of aluminium and zinc in the waste a large volume of gas is produced in the first 2.5 years. This means that the water is expelled very early from 1BMA when the concentration levels are low

Since these assumptions have a large impact on the radionuclide release calculations, a sensitivity analysis is made for both situations. In the first assumption the walls of the steel moulds and drums are totally corroded from de beginning. The cement-conditioned waste is then in direct contact with the free water in the encapsulation around the waste. This implies that the water expelled from 1BMA at early times is more contaminated.

In the second assumption, the waste does not contain aluminium and zinc. Therefore, the initial gas generation is strongly reduced. This means that the contaminated water expelled from 1BMA, to allow the gas flow and equilibrate the over-pressure, is expelled during a longer time when higher contamination levels are reached. On the other hand, the lower rate with which the water is expelled decreases the contamination rate.

The comparison was made for two cases:

- Case B1. Gas escapes through gaps between the concrete walls and the lid.
- Case ID. Initial fracture in the concrete bottom and no existing gaps between the walls and lid. In this case the concrete has a hydraulic conductivity of $8 \cdot 10^{-12}$ m/s.

The comparisons are made for non-sorbing species, since the effect will be less for sorbing species, which are retarded by sorption. The first case is the expected case and the second is an extreme case, where all the free water is expelled from the encapsulation

4.6.1 The walls of the steel moulds and drums are initially corroded.

The radionuclide release is calculated for two situations: a) (the normal case) the walls of the steel moulds and drums are intact during the first stage when water is expelled to allow the gas flow in the concrete/cement and b) no resistance in walls exists since they are totally corroded.

Figure 4-4 shows the radionuclide releases for the case B1 for non-sorbing species. For the case with totally corroded steel walls, the release rate is higher for times shorter than 20 years.

The radionuclide releases for the case ID, where an initial fracture exist in the bottom and no existing gaps between the walls and the lid, for non-sorbing species are shown in Figure 4-5. The release is significantly higher for the case with steel walls totally corroded for times less than 2.5 years. For longer times the release is slightly higher.

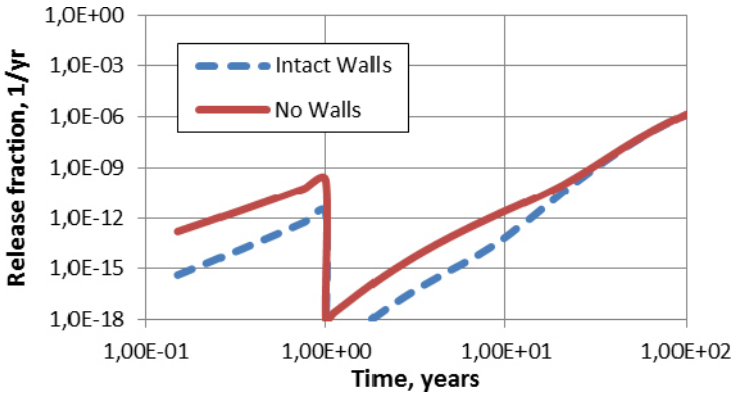

Figure 4-4. *Release fraction for a non-sorbing species for case B1 for intact and totally corroded steel walls in the moulds and drums.*

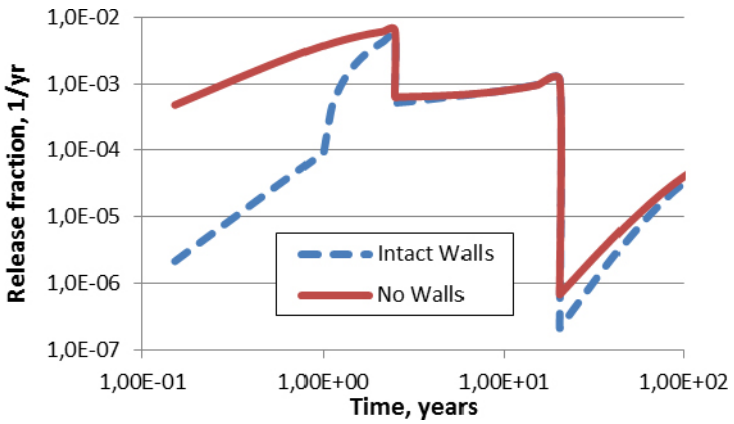

Figure 4-5. *Release fraction for a non-sorbing species for case ID for intact and totally corroded steel walls in the moulds and drums.*

4.6.2 The waste does not contain aluminium/zinc

The radionuclide release is calculated for two situations: a) (the normal case) the waste contains aluminium and zinc and b) the waste does not contain aluminium/zinc.

For case B1gas escapes through gaps between the concrete walls and the lid. 19.3 m^3 of water are initially expelled from 1BMA in order to create flow paths to allow the gas flow in the concrete. After that no more water is expelled from the encapsulation. In the case of waste containing aluminium and zinc, the gas generation rate is initially very high and it is assumed that all the water is expelled in one year. Probably the time for water expulsion is shorter, but since the start of gas generation may be different in different locations of the encapsulation, we keep the assumption of one year. For the case of waste containing no aluminium/zinc the gas generation in one year is more than three times the volume of water to be expelled, therefore it is also assumed that the time for expelling this water volume is one year. In summary, for the assumptions used in these calculations, the release of radionuclides is independent of the existence of aluminium and zinc in the waste for case B1.

For case ID, where an initial fracture exists in the bottom and with no gaps between the walls and lid, only the situation with concrete hydraulic conductivity of $8 \cdot 10^{-12}$ is studied. This is a critical case, since all free water is expelled from the encapsulation. The results in Figure 4-6 show that for waste containing aluminium and zinc the release is higher for most of the time.

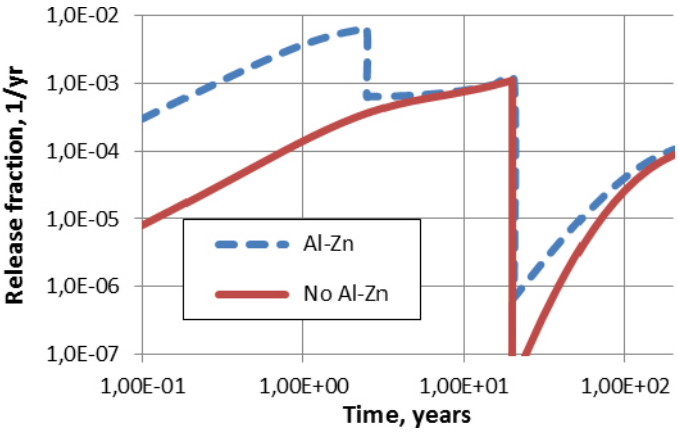

Figure 4-6. *Release fraction for a non-sorbing species for case ID for waste containing aluminium and zinc and for waste without aluminium/zinc.*

5 Gas generation in BTF

- There are three types of packages in 1BTF: concrete moulds, concrete tanks and steel drums. The steel drums will occupy the central part of each vault. The concrete tanks are used to form the walls and the concrete moulds the walls between the sections.
- The activity is initially present only in the waste. With time the concrete walls and the concrete filling between the waste packages will be contaminated mainly by diffusion. A fraction of the activity may be transported out from the packages with the water expelled by the gas generation. It is expected that the steel containers will not corrode significantly for some years.
- In 2BTF there are only concrete tanks with unsolidified resins. In this case the gas generation is small. The gas generation from 2BTF is much less than from 1BTF. For this reason the calculations are done only for 1BTF.
- The potential gas production rate of the ashes contained in the steel drums is very high initially. The gas generation starts when water reaches the ashes. The drums are not hermetically closed and gas escapes easily. During the first year enough gas is generated to expel the pore water from the concrete backfill to allow gas to flow.
- Data for gas generation rates and total gas volumes in the 1BTF and the 2BTF vaults are shown in Tables 5-1 to 5-4 for the present data (new data) and those used in Moreno et al. (2001) (old data).

Table 5-1. Gas generation rates and total gas volumes from corrosion for 1BTF.

	Initial gas generation rate, (Nm^3/y)	Old data. Initial gas generation rate, (Nm^3/y)	Total gas volumes, (Nm^3)	Old data. Total gas volumes, (Nm^3)
Packaging	9	200	482,113	110,000
Reinforcement	4	42	160,982	95,000
Waste	27,673	26,956	156,248	1,650,000
Steel	*5*	*313*	*86,999*	*1,600,000*
Aluminium/Zinc	*27,668*	*26,643*	*69,248*	*53,000*
Structures	1	26	102,953	100,000
TOTAL	**27,687**	**27,300**	**902,296**	**1,900,000**

Table 5-2. Gas generation rates and total gas volumes from corrosion and degradation for 1BTF.

	New data. Initial gas generation rate, (Nm^3/y)	Old data. Initial gas generation rate, (Nm^3/y)	New data. Total gas volumes, (Nm^3)	Old data. Total gas volumes, (Nm^3)
Corrosion				
Steel	19	581	833,048	1,905,000
Aluminium/Zinc	27,668	26,643	69,248	53,000
Microbial				
Cellulose + org	5	0.7	17,146	8,000
Resins + bitumen	10	(5.6)	151,295	(84,000)
TOTAL	**27,702**	**27,225**	**1,070,737**	**1,966,000**
No Al/Zn	**34**	**582**	**1,001,489**	**1,913,000**

Table 5-3. Gas generation rates and total gas volumes from corrosion for 2BTF.

	Initial gas generation rate, (Nm^3/y)	Old data. Initial gas generation rate, (Nm^3/y)	Total gas volumes, (Nm^3)	Old data. Total gas volumes, (Nm^3)
Packaging	2	0	689,521	0
Reinforcement	6	138	257,580	280,000
Waste	1	0	28,895	0
Steel	*1*	*0*	*28,895*	*0*
Aluminium/Zinc	*0*	*0*	*0*	*0*
Structures	2	34	136,825	140,000
TOTAL	**11**	**173**	**1,112,822**	**420,000**

Table 5-4. Gas generation rate and total gas volume from corrosion and degradation for 2BTF.

	New data. Initial gas generation rate, (Nm^3/y)	Old data. Initial gas generation rate, (Nm^3/y)	New data. Total gas volumes, (Nm^3)	Old data. Total gas volumes, (Nm^3)
Corrosion				
Steel	11	173	1,112,822	420,000
Aluminium/Zinc	0	0	0	0
Microbial				
Cellulose+org	2	2.1	29,015	31,000
Resins+bitumen	19	(20.2)	279,391	300,000
TOTAL	**32**	**175**	**1,421,228**	**751,000**
No Al/Zn	**32**	**175**	**1,421,228**	**751,000**

5.1 1BTF calculation cases

The radionuclide release is calculated for two cases:

- Case B1 where the gas escape through the backfill concrete and
- Case ID with a initial transversal fracture that crosses all the section.

5.1.1 Case B1. Gas escape through the backfill concrete

- A fraction of the water expelled to open paths for the gas flow is expelled into the gravel located at the top and bottom of the concrete structure and the floor. Another volume of water flows from the concrete filling located at the sides.
- Once paths have been opened for the gas flow no more water is expelled from the concrete. Since the initial gas generation rate is very high for the new data and the old data marginal differences are expected in the impact of the gas generation rate on the radionuclide release.

Consequences

Marginal differences are expected in the radionuclide release for new and old data because the gas generation at early times is high in both cases.

5.1.2 Case ID. Initial transversal fracture crosses all the section

- The location of the fracture is shown in Figure 5-1. When water is expelled from the repository to create paths for the gas flow the situation is similar to Case B1. The difference is that water does not flow through the concrete walls. This means that the sorption capacity (or water volume) of the concrete walls is not used to retard the transport of radionuclides.

- After paths have been created for the gas flow, no more water is expelled from the concrete.
- The water flowrate through the fracture is determined by the hydraulic gradient and the fracture geometry. For the case with a fracture crossing the modelled section transversally, the water flow rate is increased by a factor about 6 (Holmén and Stigsson 2001).

Consequences

No differences are expected in the radionuclide release induced by the gas generation, since initially the gas generation rate is determined by the corrosion of aluminium and zinc, which in both cases is very high.

5.2 Sensitivity of some assumptions made in release calculations for 1BTF

In the models used for calculating the radionuclide release, is was assumed that the steel drums are intact in the first stage when water is expelled to allow the gas flow in the cement/concrete and no contaminated water is expelled from the steel drums. Contamination may, however, escape from the concrete moulds by diffusion through the concrete walls. In this case the water is expelled in less than one year.

Another assumption was that the waste contains large amount of aluminium and zinc, which are corroded very rapidly. Due to the presence of aluminium and zinc in the waste a large volume of gas is produced in the first 2.5 years. This means that the water is expelled when the concentration levels are low.

A sensitivity analysis is made for both situations. In the first case it is assumed that the walls of the steel drums are initially corroded. The waste is then in direct contact with the buffer in the encapsulation around the waste. This implies that the water expelled at early times is more contaminated.

In the second case it is assumed that the waste does not contain aluminium and zinc. Therefore, the initial gas generation is strongly reduced. This means that the contaminated water expelled, to allow the gas flow is expelled during a longer time when higher contamination levels are reached. On the other hand, the rate at which the water is expelled is lower, decreasing the contamination rate.

The comparison was made for two cases:

- Case B1. Gas escape through the backfill concrete.
- Case ID. Initial fractures cross all section.

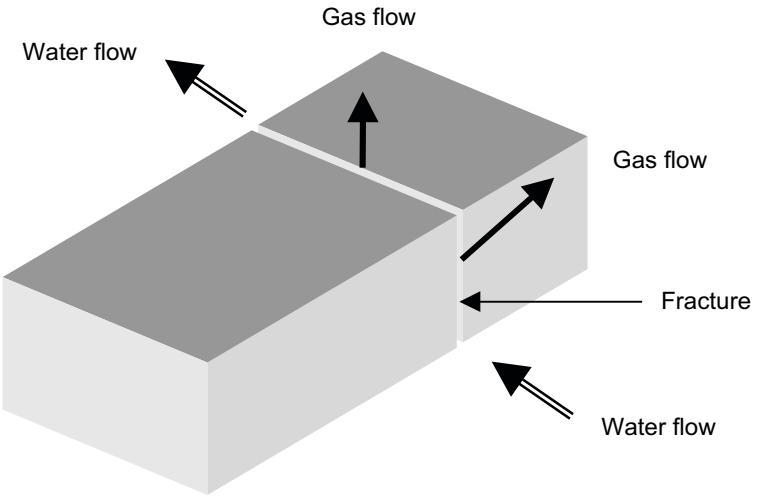

Figure 5-1. *Schematic picture showing the location of the fracture.*

The comparisons are made for non-sorbing species, since the effect will be less for sorbing species, which are retarded by sorption. The first case is the expected case and the second is an extreme case, where water flows through the repository.

5.2.1 The walls of the steel drums are initially corroded.

The radionuclide release is calculated for two situations: a) (the normal case) the walls of the steel drums are intact during the first stage when water is expelled to allow the gas flow in the concrete/ cement and b) the steel walls are totally corroded.

Figure 5-2 shows the radionuclide releases for case B1 for non-sorbing species. For the case with the steel walls totally corroded, the release rate is higher for times shorter than 20 years.

The radionuclide releases for case ID, where an initial transversal fracture crosses all the section are shown in Figure 5-3. The release is significantly higher for the case with steel walls totally corroded for times less than 1.0 year. For longer times the release is slightly higher up to 20 years and no differences are observed after that.

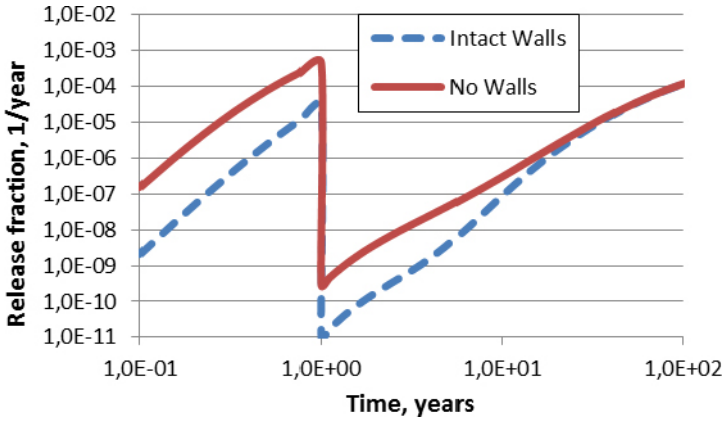

Figure 5-2. *Release fraction for a non-sorbing species for the case B1 for intact and totally corroded steel walls in the moulds and drums.*

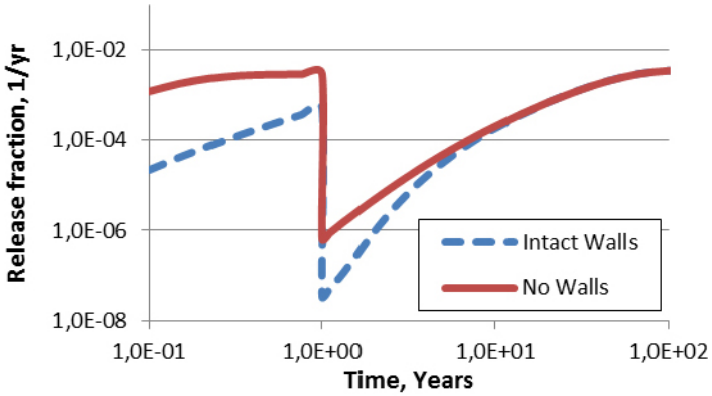

Figure 5-3. *Release fraction for a non-sorbing species for the case ID for intact and totally corroded steel walls in the moulds and drums.*

5.2.2 The waste does not contain aluminium/zinc

The radionuclide release is calculated for two situations: a) (the normal case) the waste contains aluminium and zinc and b) the waste does not contain aluminium/zinc.

For case B1, about 10 m^3 water are expelled to create flow paths for the gas flow. For waste containing aluminium and zinc, this water volume is expelled in a very short time. For waste without aluminium/zinc, the water expulsion takes a longer time. Based on the gas generation rate and water volume expelled it is assumed that water is expelled in 7 years. After that no more water is expelled from 1BTF. The results are shown in Figure 5-4. For waste containing aluminium and zinc the release is higher for short times (less than 1 year). For one to seven years the release is higher for the waste without aluminium/zinc. After that no differences are observed,

The radionuclide releases for the case ID, where an initial transversal fracture crosses all the section are shown in Figure 5-5. The release is higher for the case of waste containing aluminium and zinc for times less than 1 year. For times between one to seven years the release rate is higher for the case without aluminium/zinc. For longer times, no significant differences are observed.

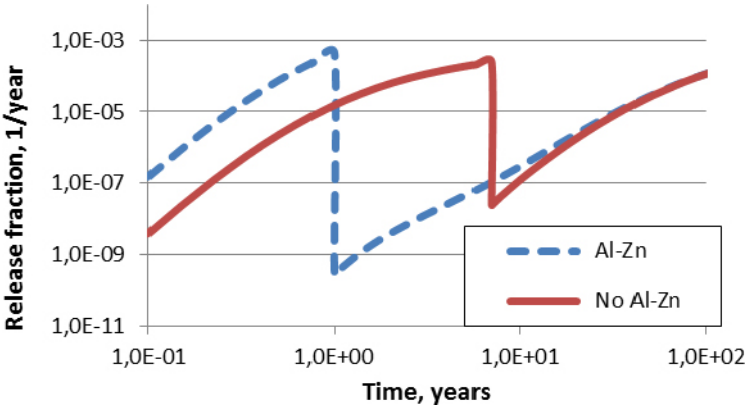

Figure 5-4. *Release fraction for a non-sorbing species for case B1 for waste containing aluminium and zinc and for waste without aluminium/zinc.*

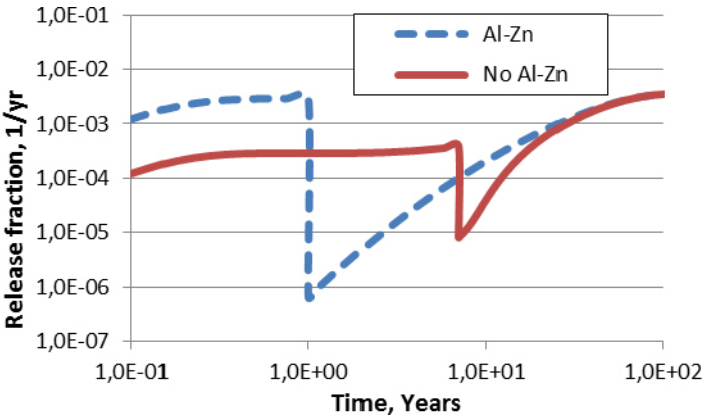

Figure 5-5. *Release fraction for a non-sorbing species for case ID for waste containing aluminium and zinc and for waste without aluminium/zinc.*

6 Summary of expelled volumes

Table 6-1 summarizes the volumes expelled in the different cases in chapters 3 to 5.

Table 6-1 Summary of water volumes expelled from the different cases.

	Volume of water expelled
Silo	**Water possible to expel is 2,000 m^3**
Case B1	
To allow gas flow	72.5 m^3 are expelled into sand and sand/bentonite on the top
To equilibrate over-pressure	200 m^3 are expelled through the outer and bottom walls
Case ID1	272 m^3 are expelled through the fracture at the bottom
Case ID2	2,070 m^3 are expelled through the fracture at the bottom
Case E1	
Case E1a: K= $8 \cdot 10^{-12}$ m/s	2,070 m^3 are expelled through outer and bottom walls
Case E1b: K= $8 \cdot 10^{-10}$ m/s	332 m^3 are expelled through outer and bottom walls
1BMA	**Water possible to expel is 3,200 m^3**
Case B1	
Water expelled to allow gas flow	19.3 m^3 are expelled into the gravel on the top
Case ID	
Case IDa: K= $8 \cdot 10^{-12}$ m/s	3,200 m^3 are expelled from 1BMA
Case IDb: K= $8 \cdot 10^{-10}$ m/s	480 m^3 are expelled from 1BMA
Case E1	
Case E1a: K = $8 \cdot 10^{-12}$ m/s	Fractures form at the upper part: 480 m^3 are expelled from 1BMA Fractures form at the bottom: 3,200 m^3 are expelled from 1BMA
Case E1b: K = $8 \cdot 10^{-10}$ m/s	480 m^3 are expelled from 1BMA
Case E2	1,600 m^3 are expelled from 1BMA
1BTF	**Water possible to expel 700 m^3**
Case B1	10 m^3 are expelled from 1BTF
Case ID	Water flow through the fracture

7 Further transport of the contamination in the expelled water

The expelled water will reside in the backfill materials where such exist and in the empty parts in the tunnels. In some extreme cases where a large water volume is expelled, some goes into the surrounding rock. In this chapter the fate of the expelled water and its contamination is discussed and compared with the earlier modelling.

The water that resides in the voids in the tunnel, being it in the backfill or the empty parts, will be carried away by the water seeping through these parts. In addition some of the contamination diffuses into the fractures in the adjacent rock and is carried away by this mechanism. The transport by water flowing in the rock is directly proportional to the flowrate through the tunnel. Table 7-1 shows that this flowrate has decreased by, approximately, a factor 9 to 268 in the different tunnels. The rate of contaminant transport in the rock and to the biosphere can be expected to decrease accordingly. Transport by the water seeping in the rock that is contaminated by diffusion also can be expected to decrease but by a smaller factor than 9–268[1]. The water that flows through the waste has also decreased considerably and will carry less nuclides if the conditions in the waste were the same. The changes of the conditions in the waste such as changed sorption coefficients are outside the scope of this report.

The volumes of water outside the concrete construction are very large. In all but a few cases the volume of expelled water is small compared to the available volume. Compare Tables 7-1 and 6-1. The exceptions are when in the Silo (Case ID2 and E1a) and 1BMA (Case IDa and E1a) all the water is expelled through a fracture in the bottom as no fractures exist in other locations. In these cases all free water is expelled and some of it will go into the fractures in the rock beneath. Then the expelled water also enters the fractures in the rock. This happens in the same way and with the same amount of water in both the old and the new data. The time of expulsion is shorter for the Silo but longer for 1BMA compared to the old case. The Silo water would then be less contaminated while the 1BMA water would become more contaminated. Therefore, for the Silo the release decreases slightly while for 1BMA the release increases slightly. The water is expelled during short time (tens of years) and only small differences in contamination is expected between old and new case.

Table 7-1. Flow of water in tunnel and through waste (data from Appendix B).

Climate scenario	Tunnel	Tunnel-Flow (m^3/y)*	Water volume in the tunnel, (m^3)	Waste-Flow (m^3/y)*
2000 AD	1BMA	0.046 (8.7)	5,600	0.008 (0.07)
2000 AD	BTF1	0.028 (7.5)	700	0.009 (2.4)
2000 AD	BTF2	0.047 (6.7)	700	0.009 (2.4)
2000 AD	Silo	0.005 (0.53)	1,800	0.005 (0.23)

* In parenthesis (Data from Moreno et al. 2001).

[1] When the transport to the seeping water is governed by diffusion the rate is proportional to the square root of the flowrate (Neretnieks et al. 2010).

8 Discussion, summary and conclusions

It was found that the new data for gas generation has a limited impact on the radionuclide release induced by the gas generation. In general the variation in the radionuclide release is well below a factor of two compared with the results from Moreno et al. (2001). This is valid for the non-sorbing radionuclides in the initial phase when water is expelled from the waste containing construction. In the subsequent period the non-sorbing and sorbing radionuclides are transported by diffusion through the barriers. In this process the remaining source is still inside the various walls of the Silo, 1BMA, BTF and waste containers. There is thus no or negligible impact on this phase by the preceding expulsion of water as by far most of the nuclides still reside inside the barriers. The non-sorbing and possibly very weakly sorbing nuclides can start diffusing from the expelled water. However, it must be remembered that the water is expelled very early when it has had no time to be much contaminated. The overall nuclide release will be dominated by diffusion at later times.

For sorbing radionuclides the impact will be even smaller since these have been retarded during the water expulsion period and reside close to the inside of the concrete walls. An exception is the case with a fracture at the bottom where the contaminated water by-passed the outer wall and the bottom-wall. The release by diffusion through the walls will therefore be much the same as in old case if the diffusion and sorption coefficients were the same. It has been outside the scope of this report to consider the impact of such changes. However, a cursory inspection of the new diffusivity and sorption data indicates that the impact of these changes will be minor.

The new gas generation rates do not change the expulsion of water contaminated with radionuclides much. In some cases more water is expelled during early times but often this happens so early that the water has had time to be less contaminated. The differences from the previous analysis are less than a factor of two using the same inventory data. The differences are summarised in Table 8-1.

The inventory has also changed. In all but a few cases the inventory of the main nuclides is about the same or lower. Only tritium has increased. In 1BMA it has increased by a factor of 80 and in 1BLA by a factor of 10. See Table 8-2. This implies that the tritium release from these vaults will increase accordingly.

The release of sorbing nuclides will not be noticeably influenced by the changes in gas production, as they have not been expelled from and through sorbing media and barriers during the few hundred years of gas generation, more than in the earlier calculations.

Table 8-1a. Summary of the results for expelled water from the Silo.

Case B1 – Gas escapes through the evacuation pipes in the concrete lid	
Step 1: water is expelled to allow gas flow.	*Similar radionuclide release using the old and new data.*
Step 2: water is expelled to equilibrate the pressure.	*Small increase of radionuclide release due to the new bentonite conductivity data.*
Case ID1 – Initial fracture in the bottom of the Silo and gas escape through the evacuation pipes in the concrete lid	
	The same radionuclide release for new and old data.
Case ID2 – Initial fracture in the bottom and no evacuation pipes in the concrete lid	
	The radionuclide release is slightly less for the new data (about 15% less).
Case E1 – Concrete lid without evacuation pipes	
Case E1a: K= 8·E–12 m/s.	*Less radionuclide release using the new data (about 15% less).*
Case E1b: K= 8·E–10 m/s.	*The same radionuclide release for new and old data.*

Table 8-1b. Summary of the results for expelled water from 1BMA.

Case B1 – Gas escapes through gaps between the concrete walls and the lid	
Water is expelled to allow gas flow.	*The same radionuclide release for new and old data.*
Case ID – Initial fracture in the concrete bottom and no existing gaps between the walls and lid	
Case IDa: K= $8 \cdot 10^{-12}$ m/s	*Higher radionuclide release using the new data (about 25% higher).*
Case IDb: K= $8 \cdot 10^{-10}$ m/s	*The same radionuclide release for new and old data.*
Case E1 – No existing gaps between the concrete walls and the lid	
E1a: K = $8 \cdot 10^{-12}$ m/s	*Fractures form in the upper part: The same radionuclide release for new and old data.*
	Fractures form at the bottom: higher radioactivity release using the new data (about 25% higher).
E1b: K = $8 \cdot 10^{-10}$ m/s	*The same radionuclide release for new and old data.*
Case E2 – No existing gaps between the concrete walls and the lid and the space between the waste containers is filled with porous concrete	
	The same radionuclide release for new and old data.

Table 8-1c. Summary of the results for expelled water from 1BTF.

Case B1 – Gas escape through the backfill concrete	
	The same radionuclide release for new and old data.
Case ID – Initial transversal fracture crosses all the section	
	The same radionuclide release for new and old data.

Table 8.2. Changes in inventory of some important nuclides. Old inventory (Used in R-01-11) and new inventory data (Appendix B).

Nuclide	Half-life, years	Silo	1BMA	1BTF	2BTF	1BLA
^{3}H						
Old data, 2030	12.3	5.80E+11	3.30E+10	3.30E+09	5.30E+09	6.60E+08
Old data 2075		4.60E+10	2.62E+09	2.62E+08	4.21E+08	5.24E+07
New data 2075		7.30E+09	2.10E+11	1.30E+08	6.20E+07	5.10E+08
Ratio new/old		0.16	80.18	0.50	0.15	9.74
^{14}C org						
Old data	5,730	1.80E+12	1.70E+11	1.80E+11	3.00E+10	3.30E+07
New data		6.30E+11	1.40E+11	1.10E+10	5.30E+09	8.10E+07
Ratio new/old		0.35	0.82	0.06	0.18	2.45
^{36} Cl						
Old data	301,000	4.70E+10	3.40E+09	3.00E+08	5.40E+08	8.20E+07
New data		1.00E+09	3.40E+08	3.10E+07	1.30E+07	2.20E+07
Ratio new/old		0.02	0.10	0.10	0.02	0.27
^{129}I						
Old data	1.60E+07	1.40E+09	1.00E+08	9.10E+06	1.60E+07	2.50E+06
New data		8.70E+08	1.50E+08	1.30E+07	1.40E+07	4.30E+05
Ratio new/old		0.62	1.50	1.43	0.88	0.17

References

SKB's (Svensk Kärnbränslehantering AB) publications can be found at www.skb.se/publications.

Abarca E, Idiart A, Manuel de Vries L, Silva O, Molinero J, von Schenck H, 2013. Flow modelling on the repository scale for the safety assessment SR-PSU. SKB TR-13-08, Svensk Kärnbränslehantering AB.

Firestone R B, Baglin C M, Chu S Y F, 1998. Table of isotopes: 1998 update with CD-Rom. New York: Wiley.

Holmén J G, Stigsson M, 2001. Modelling of future hydrogeological conditions at SFR. SKB R-01-02, Svensk Kärnbränslehantering AB.

Jörg G, Bühnemann R, Hollas S, Kivel N, Kossert K, Van Winckel S, Gostomski C L, 2010. Preparation of radiochemically pure (79)Se and highly precise determination of its half-life. Applied Radiation and Isotopes 68, 2339–2351.

Lindgren M, Pettersson M, Karlsson S, Moreno L, 2001. Project SAFE. Radionuclide release and dose from the SFR repository. SKB R-01-18, Svensk Kärnbränslehantering AB.

Moreno L, Skagius K, Södergren S, Wiborgh M, 2001. Project SAFE. Gas related processes in SFR. SKB R-01-11, Svensk Kärnbränslehantering AB.

Neretnieks I, Liu L, Moreno L, 2010. Mass transfer between waste canister and water seeping in rock fractures. Revisiting the Q-equivalent model. SKB TR-10-42, Svensk Kärnbränslehantering AB.

Pettersson M, Elert M, 2001. Characterisation of bitumenised waste in SFR 1. SKB R-01-26, Svensk Kärnbränslehantering AB.

Schrader H, 2004. Half-life measurements with ionization chambers – a study of systematic effects and results. Applied Radiation and Isotopes 60, 317–323.

SKB, 2001. Project SAFE. Compilation of data for radionuclide transport analysis. SKB R-01-14, Svensk Kärnbränslehantering AB.

SKB, 2013. Låg- och medelaktivt avfall i SFR – Referensinventarium för avfall 2013. SKB R-13-37, Svensk Kärnbränslehantering AB.

SKB, 2014a. Data report for the safety assessment SR-PSU. SKB TR-14-10, Svensk Kärnbränslehantering AB.

SKB, 2014b. Initial state report for the safety assessment SR-PSU. SKB TR-14-02, Svensk Kärnbränslehantering AB.

Thomson G, Miller A, Smith G, Jackson D, 2008a. Radionuclide release calculations for SAR-08. SKB R-08-14, Svensk Kärnbränslehantering AB.

Thomson G, Herben M, Lloyd P, Rose D, Smith C, Barraclough I, 2008b. Implementation of project Safe in Amber. Verification study for SFR 1 SAR-08. SKB R-08-13, Svensk Kärnbränslehantering AB.

Wiborgh M, Höglund L O, Pers K, 1986. Gas formation in a L/ILW repository and gas transport in the host rock. Nagra Technical Report NTB 85-17, Nagra, Switzerland.

Appendix A

Gas formation

Updated by Maria Lindgren, Kemakta Konsult AB.

A.1 Gas formation processes

Gas can be formed in the repository by hydrogen evolving corrosion of metals, by microbial degradation of organic materials and by radiolytic decomposition of water. Gas formation due to radiolytic decomposition of water has been shown to be negligible compared to gas produced by corrosion throughout the lifetime of the repository and in all repository parts of SFR 1 (Moreno et al. 2001). Hence, it is omitted in the calculations below.

A.1.1 Metal corrosion

The major metal present in the repository is steel, but the waste also contains other metals such as aluminium and zinc.

Steel is present in all repository parts. Hydrogen evolving corrosion can occur only in the absence of dissolved oxygen. This implies that anaerobic corrosion will start when aerobic corrosion or another oxygen consuming reaction, such as microbial activity has consumed the oxygen initially present.

Under anaerobic conditions, the amount of hydrogen evolved can be estimated by the following overall reaction for corrosion of steel, for which the formation of magnetite is the end product (Höglund and Bengtsson 1991).

$$3Fe(s) + 4H_2O \rightarrow Fe_3O_4(s) + 4H_2(g)$$

Aluminium is present in the waste in all parts of the repository. Due to the large amount of concrete, the water in contact with the aluminium waste will be alkaline. Aluminium is not thermodynamically stable in water, but has a very dense protective oxide layer. However, in alkaline environments this oxide layer will dissolve and a rapid corrosion of aluminium yielding hydrogen can take place according to the reaction (Höglund and Bengtsson 1991):

$$2Al(s) + 2OH^- + 4H_2O \rightarrow 2AlO(OH)_2^- + 3H_2(g)$$

or alternatively

$$2Al(s) + 2OH^- + 2H_2O \rightarrow 2AlO_2^- + 3H_2(g)$$

In calculating the gas formation rates due to corrosion all corroding parts, except reinforcements in concrete packages and concrete structures, are assumed to have a planar geometry. Gas formation by corrosion of reinforcement bars considers the shrinking surface, which is a function of the time.

The estimated gas generation rates from corrosion of metals in waste packages and concrete structures are calculated using the amounts and dimensions of construction materials as given in references given in Table A-1. The inventory of the waste does not separate aluminium and zinc. Quantities given as the sum of aluminium and zinc have been treated as aluminium.

The corrosion rate of 0.05 μm/year has been used for iron and steel (SKB 2014a). For aluminium, the corrosion rate has been assumed to be 1 mm/year (SKB 2014a).

Table A-1. References used for amounts and dimensions of corroding materials.

	References used for amounts and dimensions of corroding materials	
	SFR 1 (Silo, 1BMA, 1BTF, 2BTF and 1BLA)	SFR 3 (2BMA, 2-5BLA, BRT)
Waste	Inventory report (SKB, 2013)[1]	Inventory report (SKB, 2013)[1]
Packagings	Initial state report (SKB 2014b)	Initial state report (SKB 2014b)
Structures	Moreno et al. 2001, Appendix A	Initial state report (SKB 2014b)

[1] Values taken from an earlier version of SKB 2013. In this report the values from the earlier version has been used. The conclusions drawn are judged not to be affected.

A.1.2 Microbial degradation of organic materials

Organic materials are present in the waste in SFR. These materials may be digested by microorganisms. Examples of microbially degradable materials are cellulose, ion exchange resins with organic matrices, different scrap material and bitumen. The result of microbial degradation in SFR may be unwanted effects, such as the formation of gas.

The chemical environment significantly influences the rate of microbial degradation, where optimal conditions for most microorganisms are at a pH close to neutral, a temperature of 25–30°C, and absence of biotoxic substances. However, different microorganisms possess a remarkable ability to adapt to different environments. Therefore, microbial activity and gas formation cannot be excluded even if strongly alkaline conditions are expected in the waste packages after saturation of the repository.

Under aerobic conditions, microbial degradation of organics will consume oxygen and produce carbon dioxide. Aerobic corrosion of the large amounts of steel in the repository will also consume oxygen. Due to these processes, the rather small amounts of oxygen initially present after closure of the repository is assumed to be totally consumed a short time after the closure and anaerobic conditions will be established.

Under anaerobic conditions, other oxidants such as nitrate, sulphate and carbon dioxide will participate in the microbial degradation process. A simplified reaction formula for the degradation of an arbitrary organic compound can be written as:

$$C_{org} + \text{Oxidant} \rightarrow C^{*}_{org} + H_2 + CO_2 + CH_4 + \text{Reducing agent}$$

Gas formation rates for microbial degradation of organic materials are relatively sparse. The type of organic substrate as well as the surface area available for microbial attack is important for the degradation rate. The organic material can be divided into two groups, cellulose material with a large surface to volume ratio and other organic materials with a low surface to volume ratio. Other organic material includes ion exchange resins, plastic, rubber etc.

Based on data on the organic content in the waste from SKB (2013)[2], the contribution to the total amount of gas from microbial degradation of cellulose has been calculated. Conservative estimations of the degradation of ion-exchange resins, bitumen and plastics have also been made. In the calculations, degradation rates for cellulose corresponding to complete degradation in a little less than 200 years is assumed (37/0.2=185years). This results in a degradation rate of 0.2 mole/kg,year and a gas formation rate of about 2 l/kg,year, assuming that 50% of the gases are inert, see Table A-2.

In the literature, data on the microbial degradation of bitumen, ion-exchange resins and plastics are scarce. The few experiments found imply that these are very slow processes. In the calculations it is assumed that 0.002 mole/kg,year is degraded, corresponding to a degradation of all material in 15,000 years and a gas formation rate of 0.02 l/kg,year assuming that 50% of the gases are inert, see Table A-2.

Table A-2. Gas formation rates and maximum yields for microbial degradation of cellulose and other organics (Wiborgh et al. 1986).

	Cellulose	Other organics
Rate, [mole gas/year, kg organic]	0.2	0.002
Maximum yield, [mole gas/kg organic]	37	30

A.2 Gas formation in SFR due to metal corrosion

A.2.1 The Silo

The results for the Silo are given in Figure A-1, Figure A-2 and in Table A-3.

The gas formation rates are calculated for structures, packaging, reinforcement in packaging and waste separately. Packaging includes metals in the packaging of the waste, excluding reinforcement

[2] Values taken from an earlier version of SKB 2013. In this report the values from the earlier version has been used. The conclusions drawn are judged not to be affected.

bars in concrete packaging, which are shown separately. The category waste in the figures includes steel and aluminium in the waste. Structures include gas formed from corrosion of reinforcement bars in the concrete structures of the repository.

For the first 2.5 years corrosion of aluminium in the waste will dominate the gas formation, see Figure A-1.

Table A-3. Initial gas formation rates and maximum theoretical gas volume that can be formed due to corrosion of metals in the Silo.

	Initial gas formation rate, [m³/year]	Total gas volumes, [m³]
Packaging	22	1,107,305
Reinforcement	13	755,012
Waste	4,638	660,456
Steel	*10*	*649,029*
Aluminium	*4,628*	*11,427*
Structures	4	241,703
Total	**4,677**	**2,764,476**

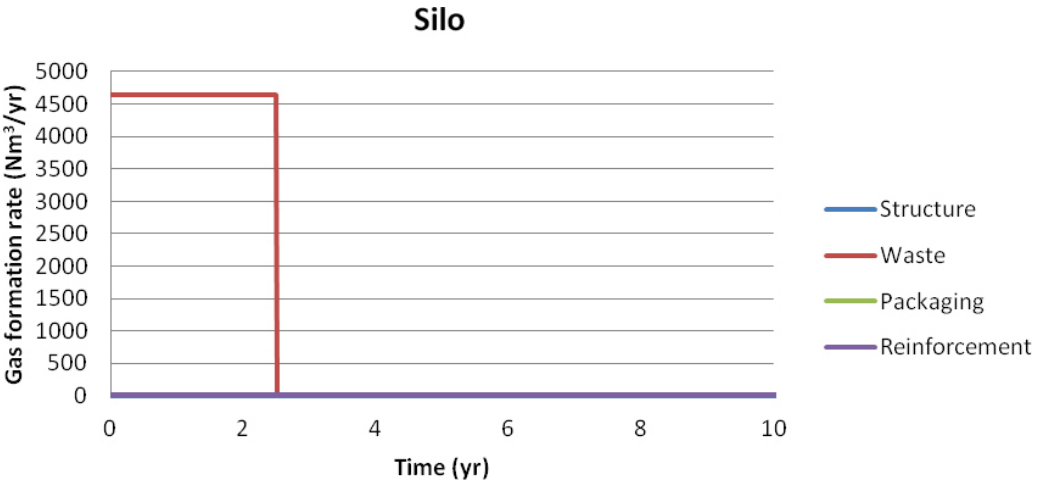

Figure A-1. *Gas formation rates due to corrosion in the Silo, [Nm³/year]. 0–10 years.*

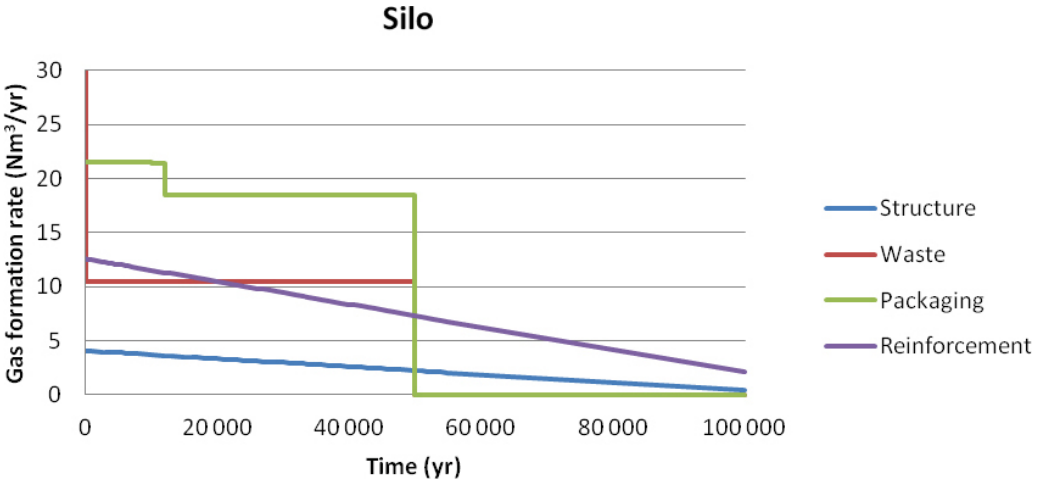

Figure A-2. *Gas formation rates due to corrosion in the Silo, [Nm³/year]. 0–100,000 years.*

A.2.2 The 1BMA vault

The results are given in Figure A-3, Figure A-4 and in Table A-4.

The gas formation rates are calculated for packaging (steel), reinforcement (steel), waste (steel and aluminium) and structures (steel) separately.

For the first 2.5 years corrosion of aluminium in the waste will dominate the gas formation, see Figure A-3.

Table A-4. Initial gas formation rates and maximum theoretical gas volume that can be formed due to corrosion of metals in 1BMA.

	Initial gas formation rate, [m³/year]	Total gas volumes, [m³]
Packaging	16	701,177
Reinforcement	10	627,376
Waste	4,448	307,039
Steel	*6*	*295,553*
Aluminium	*4,442*	*11,486*
Structures	3	214,522
Total	**4,477**	**1,850,114**

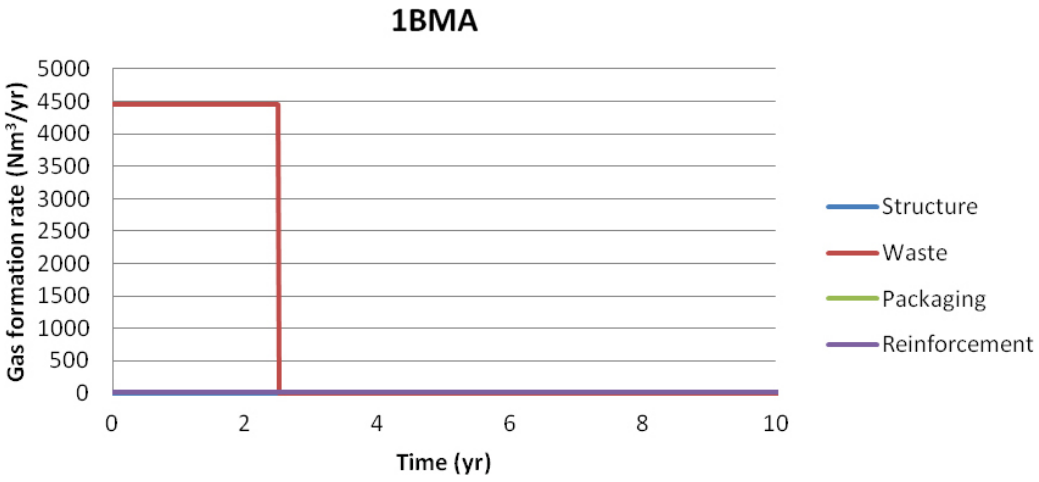

Figure A-3. *Gas formation rates due to corrosion in 1BMA, [Nm³/year]. 0–10 years.*

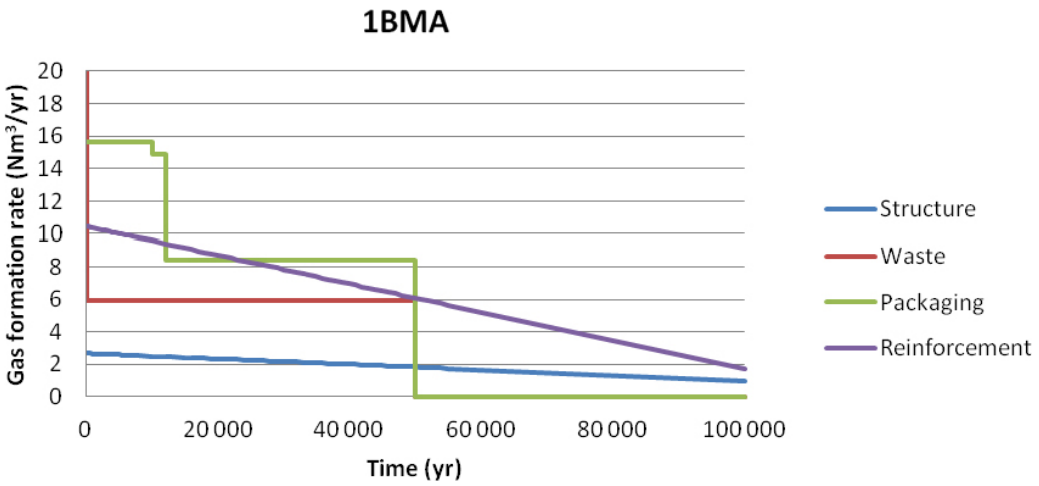

Figure A-4. *Gas formation rates due to corrosion in 1BMA, [Nm³/year]. 0–100,000 years.*

A.2.3 The BTF vaults

The results are given in Figure A-5 to Figure A-8 and in Table A-5 and Table A-6. In the BTF vaults the only concrete structures are the bottom and lids.

For 1BTF the gas formation rates are calculated for packaging (steel), reinforcement (in packaging), waste (steel and aluminium) and structures (reinforcement) separately.

For the first years, the corrosion of aluminium in the waste will dominate the gas formation in 1BTF, see Figure A-5.

The high rate for gas formation from aluminium is explained by the large amount of aluminium present in the 1BTF vault. However, since the aluminium is completely depleted after a few years, the total gas volume formed is small, see Table A-5 .

Table A-5. Initial gas formation rates and maximum theoretical gas volume that can be formed due to corrosion of metals in 1BTF.

	Initial gas formation rate, [m³/year]	Total gas volumes, [m³]
Packaging	9	482,113
Reinforcement	4	160,982
Waste	27,673	156,248
Steel	*5*	*86,999*
Aluminium	*27,668*	*69,248*
Structures	1	102,953
Total	**27,687**	**902,296**

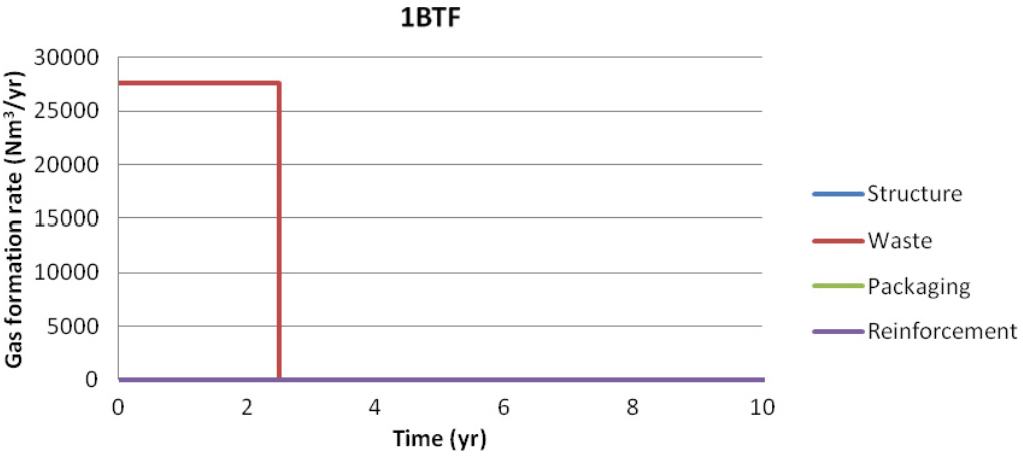

Figure A-5. *Gas formation rates due to corrosion in 1BTF, [Nm³/year]. 0–10 years.*

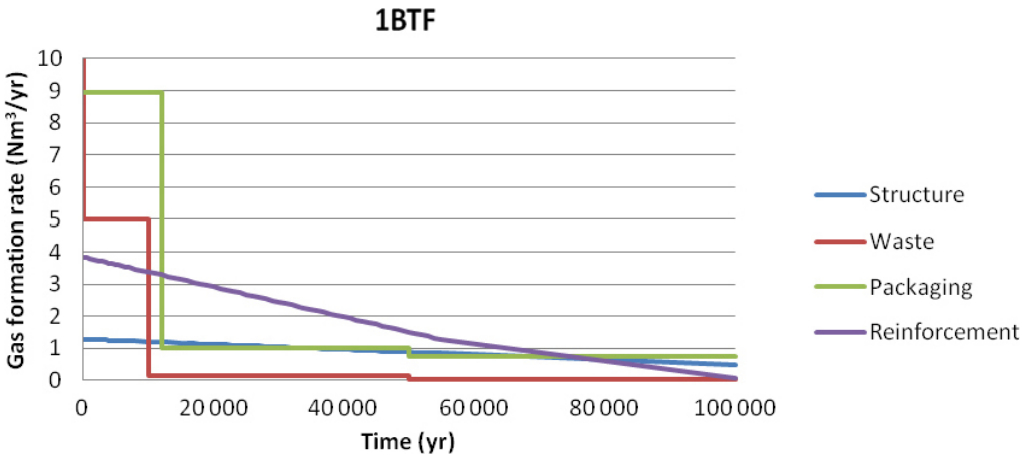

Figure A-6. *Gas formation rates due to corrosion in 1BTF, [Nm³/year]. 0–100,000 years.*

Table A-6. Initial gas formation rates and maximum theoretical gas volume that can be formed due to corrosion of metals in 2BTF.

	Initial gas formation rate, [m³/year]	Total gas volumes, [m³]
Packaging	2	689,521
Reinforcement	6	257,580
Waste	1	28,895
Steel	*1*	*28,895*
Aluminium	*0*	*0*
Structures	2	136,825
Total	**10**	**1,112,822**

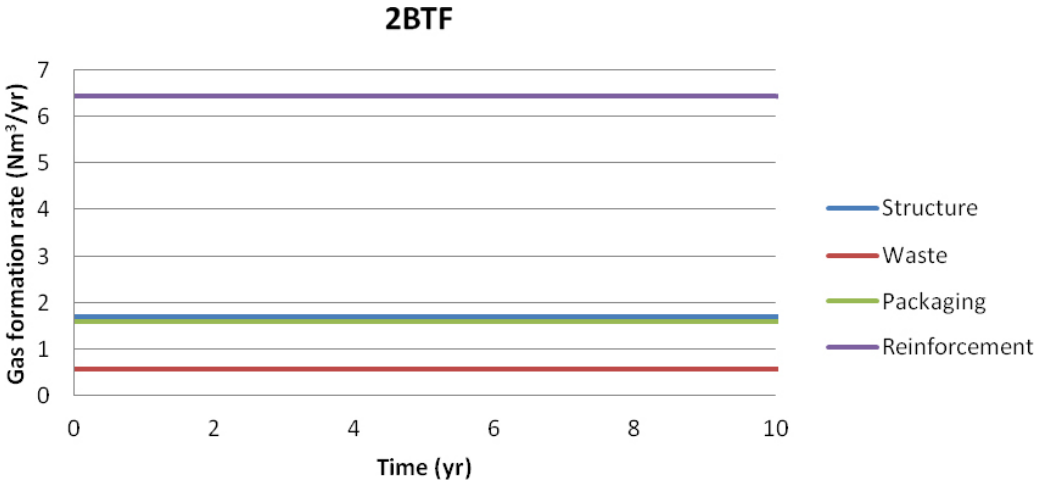

Figure A-7. Gas formation rates due to corrosion in 2BTF, [Nm³/year]. 0–10 years.

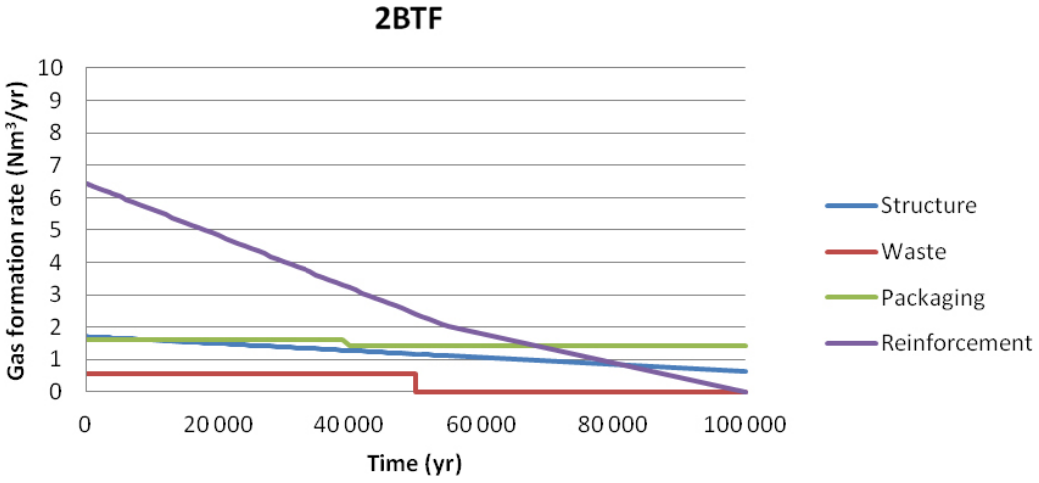

Figure A-8. Gas formation rates due to corrosion in 2BTF, [Nm³/year]. 0–100,000 years.

A.2.4 The BLA vault

The results are given in Figure A-9, Figure A-10 and in Table A-7. In the 1BLA vault the only concrete structure is the bottom which is made of reinforced concrete.

For the first 2.5 years corrosion in 1BLA aluminium in the waste will dominate the gas formation, see Figure A-9.

The high rate for gas formation from aluminium is explained by the large amount of aluminium present in the BLA vault. However, since the aluminium is completely depleted after 2.5 years, the total gas volume formed is small, see Table A-7.

Table A-7. Initial gas formation rates and maximum theoretical gas volume that can be formed due to corrosion of metals in 1BLA.

	Initial gas formation rate, [m³/year]	Total gas volumes, [m³]
Packaging	20	658,415
Reinforcement	0	0
Waste	29,970	1,311,695
steel	*27*	*1,236,390*
aluminium	*29,942*	*75,305*
Structures	1	50,353
Total	**29,990**	**2,020,463**

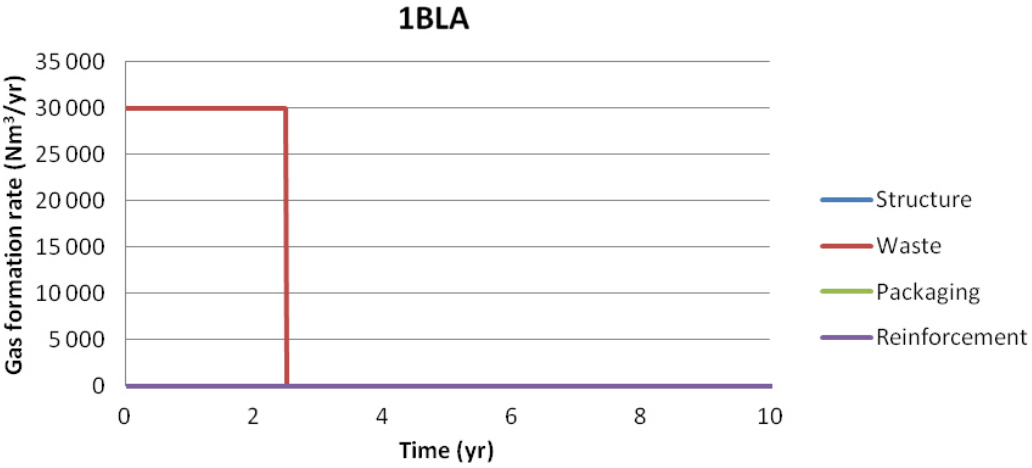

Figure A-9. *Gas formation rates due to corrosion in 1BLA, [Nm³/year]. 0–10 years.*

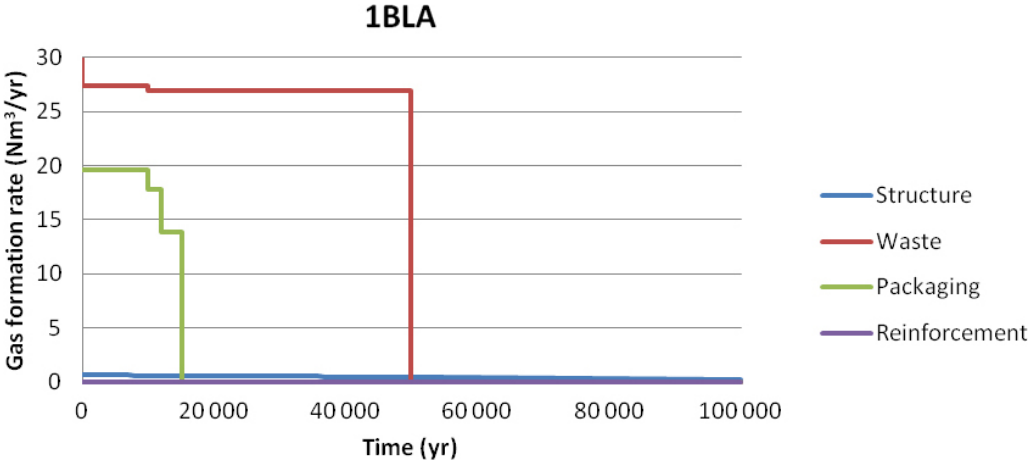

Figure A-10. *Gas formation rates due to corrosion in 1BLA, [Nm³/year]. 0–100,000 years.*

A.2.5 The 2BMA vault

Results for 2BMA, the intermediate level waste vault in SFR 3, are given in Figure A-11, Figure A-12 and in Table A-8. In the 2BMA the structure concrete structure is made without reinforcement.

For the first 2.5 years corrosion in 2BMA aluminium in the waste will dominate the gas formation, see Figure A-11.

Table A-8. Initial gas formation rates and maximum theoretical gasvolume that can be formed due to corrosion of metals in 2BMA.

	Initial gas formation rate, [m³/year]	Total gas volumes, [m³]
Packaging	44	3,896,773
Reinforcement	2	92,222
Waste	102,456	6,740,074
Steel	*132*	*6,484,475*
Aluminium	*102,324*	*255,600*
Structures	0	0
Total	**102,502**	**10,729,070**

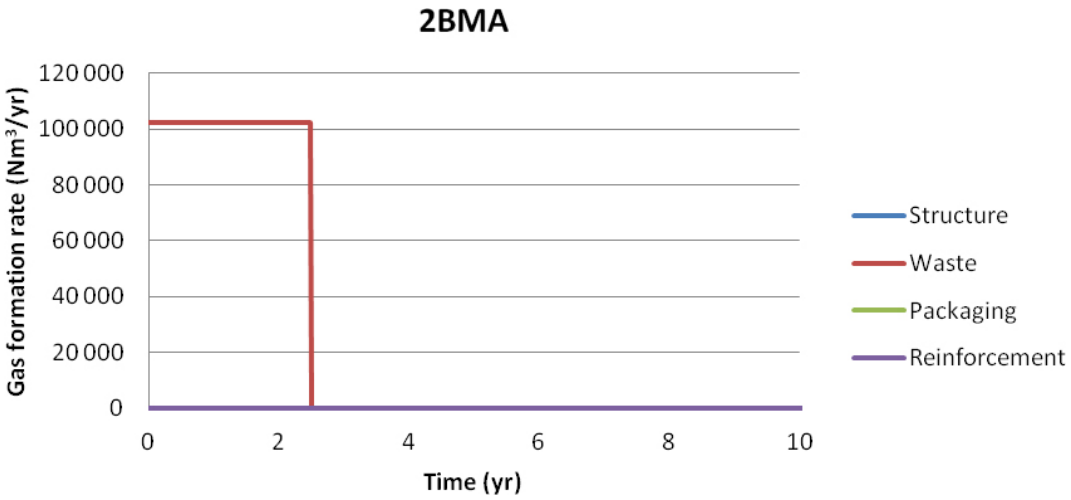

Figure A-11. *Gas formation rates due to corrosion in 2BMA, [Nm³/year]. 0–10 years.*

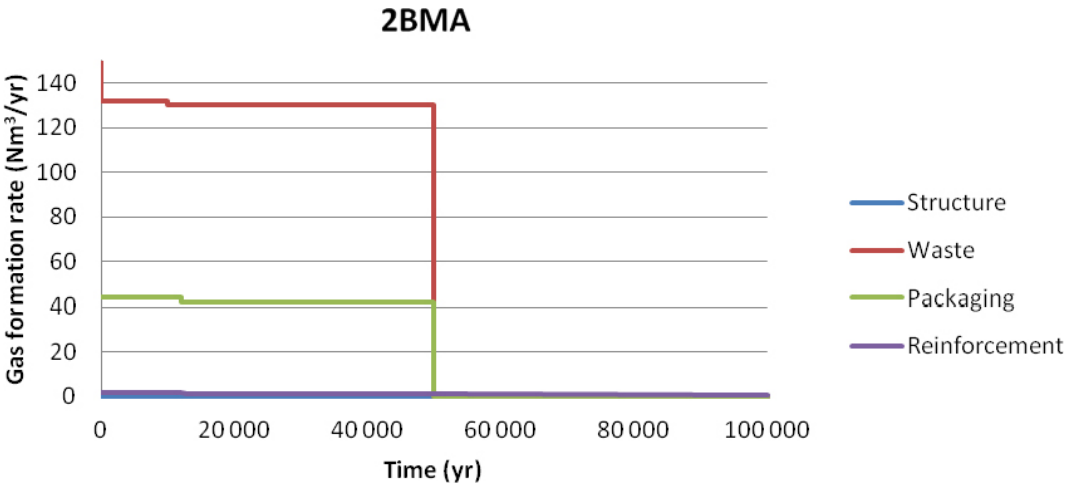

Figure A-12. *Gas formation rates due to corrosion in 2BMA, [Nm³/year]. 0–100,000 years.*

A.2.6 The 2-5BLA vaults

Results for 2-5BLA, the low level waste vaults in SFR 3, are given in Figure A-13, Figure A-14 and in Table A-9. In the 2-5BLA vaults the only concrete structures are the bottom plates which are made of reinforced concrete. The amount of reinforcement is assumed to be the same per meter as in 1BLA.

For the first 2.5 years corrosion in 2-5BLA aluminium in the waste will dominate the gas formation, see Figure A-13.

Table A-9. Initial gas formation rates and maximum theoretical gasvolume that can be formed due to corrosion of metals in 2-5BLA.

	Initial gas formation rate, [m³/year]	Total gas volumes, [m³]
Packaging	139	6,387,756
Reinforcement	0	0
Waste	258,154	13,142,036
Steel	*252*	*12,495,457*
Aluminium	*257,903*	*646,580*
Structures	4	346,176
Total	**258,298**	**19,875,969**

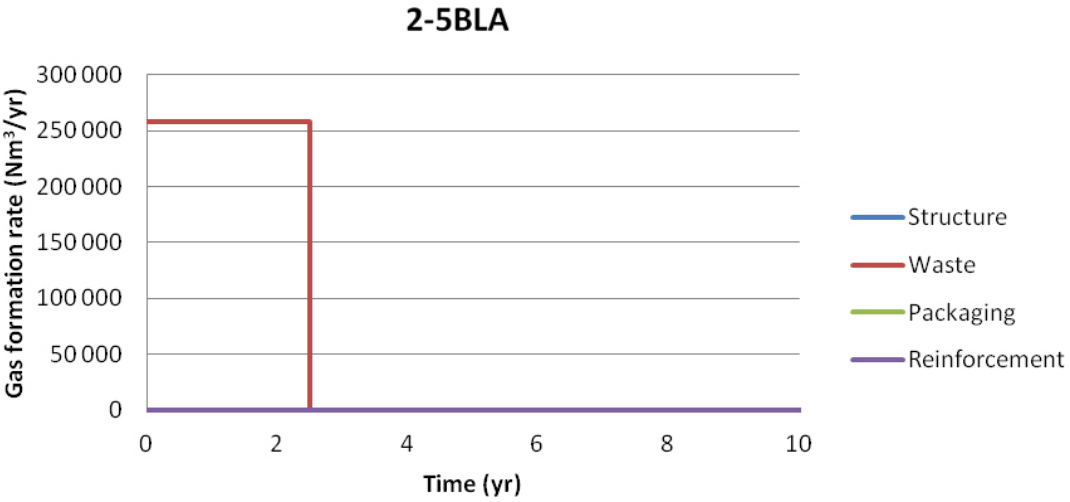

Figure A-13. *Gas formation rates due to corrosion in 2-5BLA, [Nm³/year]. 0–10 years.*

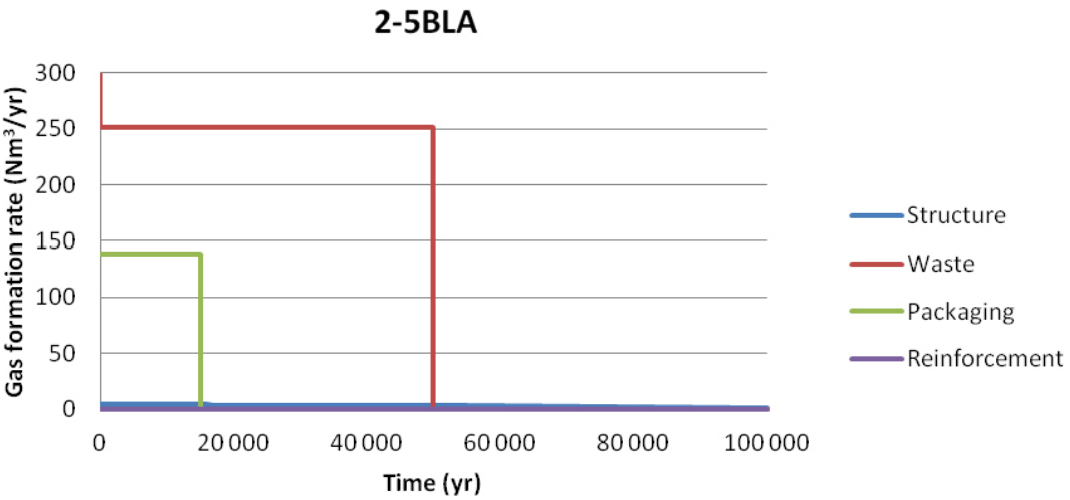

Figure A-14. *Gas formation rates due to corrosion in 2-5BLA, [Nm³/year]. 0–100,000 years.*

A.2.7 The BRT vault

Results for BRT, the vault for BWR reactor vessels in SFR 3, are given in Figure A-15 and Table A-10. No reinforcement in the concrete structure has been accounted for.

Table A-10. Initial Initial gas formation rates and maximum theoretical gasvolume that can be formed due to corrosion of metals in BRT (not corrosion rate for stainless steel).

	Initial gas formation rate, [m³/year]	Total gas volumes, [m³]
Packaging	0	0
Reinforcement	0	0
Waste	1	3,016,466
Steel	*1*	*3,016,466*
Aluminium	*0*	*0*
Structures	0	0
Total	**1**	**3,016,466**

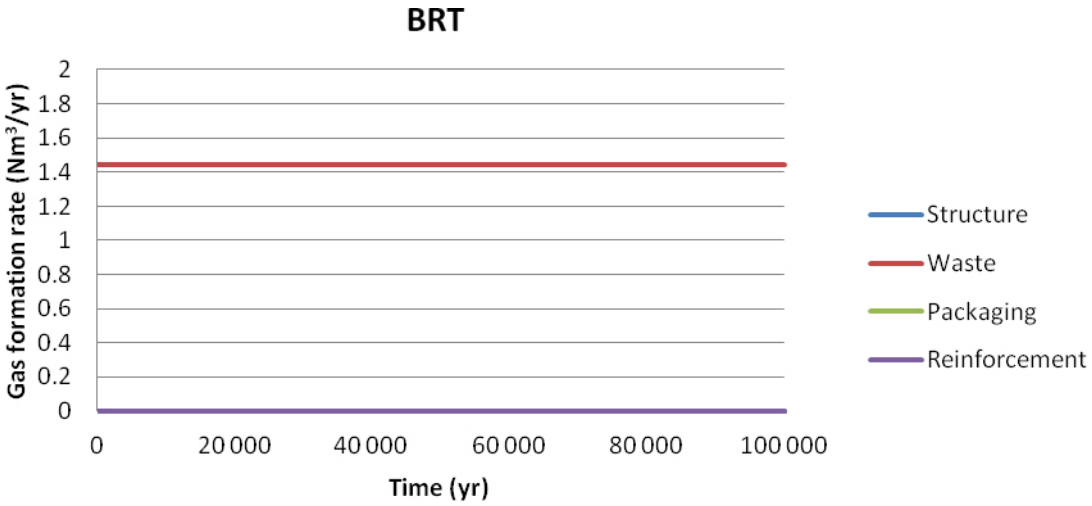

Figure A-15. *Gas formation rates due to corrosion in BRT, [Nm³/year]. 0–100,000 years.*

A.3 Gas formation in SFR due to microbial degradation of organic material

The initial gas formation rates and the maximum theoretical gas volumes that can be formed due to microbial degradation of organic material in the different repository parts in SFR are given in Table A-11.

The gas formation rates have been calculated for cellulose and other organics, such as plastics, ion exchange resins and bitumen. However, material such as ion-exchange resins and bitumen are thought to degrade so slowly that the gas formation rate can be neglected. Therefore the rates for resins and bitumen are shown separately in Table A-11 and in the tables given in the summary, see Section A.4.

Table A-11. Initial gas formation rates and maximum theoretical gas volume that can be formed due to microbial degradation of organic material in SFR.

Material	Initial gas formation rate, [m³/year]								
	Silo	1BMA	1BTF	2BTF	1BLA	2BMA	2-5BLA	BRT	Total
Cellulose	54	269	4	0	623	3,833	5,828	0	10,602
Other org	1	6	1	2	30	51	350	0	439
(Resins+bitumen)	89	72	10	19	5	10	0	0	204

	Maximum theoretical gas volume, [m³]								
	Silo	1BMA	1BTF	2BTF	1BLA	2BMA	2-5BLA	BRT	Total
Cellulose	10,076	49,759	672	0	115,275	709,067	1,078,113	0	1,961,337
Other org	17,113	90,777	16,474	29,015	447,159	763,197	5,244,876	0	6,589,716
(Resins+bitumen)	1,329,038	1,079,234	151,295	279,391	69,730	148,269	0	0	3,056,149

A.4 Summary of gas formation rates and gas volumes

A summary of gas formation rates and total volumes of gas formed in the different repository parts in SFR due to different processes are given in The gas generation rate is initially totally dominated by corrosion of aluminium. The total amount of gas generated is dominated by corrosion of steel.

Table A-12 and Table A-13. The gas generation rate is initially totally dominated by corrosion of aluminium. The total amount of gas generated is dominated by corrosion of steel.

Table A-12. Gas formation rates for different repository parts in SFR.

	Initial gas formation rate, [m³/year]								
	Silo	1BMA	1BTF	2BTF	1BLA	2BMA	2-5BLA	BRT	Total
Corrosion									
Steel	49	35	19	10	48	177	395	1	735
Al/Zn	4,628	4,442	27,668	0	29,942	102,324	257,903	0	426,907
Microbially									0
Cellulose	54	269	4	0	623	3,833	5,828	0	10,611
Other org	1	6	1	2	30	51	350	0	441
(Resins+bitumen)	89	72	10	19	5	10	0	0	204
Total	**4,821**	**4,824**	**27,702**	**31**	**30,647**	**106,395**	**264,475**	**1**	**438,897**

Table A-13. Total gas volumes for different repository parts in SFR.

	Total gas volumes, [m³]				
	Silo	**1BMA**	**1BTF**	**2BTF**	**1BLA**
Corrosion					
Steel	2,753,049	1,838,628	833,047	1,112,822	2,020,463
Al/Zn	11,427	11,486	69,248	0	75,305
Microbially					
Cellulose	10,076	49,759	672	0	115,275
Other org	17,113	90,777	16,474	29,015	447,159
(Resins+bitumen)	1,329,038	1,079,234	151,295	279,391	69,730

	Total gas volumes, [m³]			
	2BMA	**2-5BLA**	**BRT**	**Total**
Corrosion				
Steel	10,473,470	19,229,389	3,016,466	41,277,332
Al/Zn	255,600	646,580	0	1,069,646
Microbially				
Cellulose	709,067	1,078,113	0	1,961,337
Other org	763,197	5,244,876	0	6,589,716
(Resins+bitumen)	148,269	0	0	3,056,149

Appendix B

Data used in SR-PSU

Klas Källström, SKB

B.1 Material data

Table B-1. Effective diffusivity, m^2/s.

Material	Value	Reference	Old value used in R-01-11
Structural concrete	3.0E–12	Thomson et al. 2008a	1.0E–11
Porous concrete	3.0E–10	Thomson et al. 2008a	1.0E–10
Gravel and sand	6.0E–10	Thomson et al. 2008a	6.0E–10
Cement in conditioning	3.0E–10	Thomson et al. 2008a	1.0E–10
Bentonite	4.6E–10	Thomson et al. 2008a	1.0E–10 (dry)
Sand/bentonite	5.0E–10	Thomson et al. 2008a	1.0E–10 (dry)
Bitumen	2.0E–09		–
Water	2.0E–09	Thomson et al. 2008a	2.0E–9

The values for concrete corresponds for new concrete. For old concrete 3.0E–11 m^2/s is used.
The values for bitumen is not a realistic value.

Table B-2. Porosity.

Material	Value	Reference	Old value used in R-01-11
Structural concrete	0.15	Thomson et al. 2008a	0.15
Porous concrete	0.30	SKB 2001	0.3
Gravel and sand	0.30	Thomson et al. 2008a	0.3
Cement in conditioning	0.28	Thomson et al. 2008a	0.2
Bentonite	0.61	SKB 2001	0.61 (dry)
Sand/bentonite	0.25	Thomson et al. 2008a	0.25 (dry)
Bitumen	0.10	Thomson et al. 2008b	0
Water	1.00	Thomson et al. 2008a	1.0

Table B-3. Material density, kg/m^3.

Material	Value	Old value used in R-01-11
Structural concrete	2,529.4	2,300
Porous concrete	2,428.6	2,000
Gravel and sand	2,700.0	2,190
Cement in conditioning	2,250.0	2,300
Bentonite	2,692.3	1,050 (dry)
Sand/bentonite	2,666.7	2,000 (dry)
Bitumen	1,030.0	1,030

Table B-4. Hydraulic conductivity, m/s.

Material	Value	Reference	Old value used in R-01-11
Structural concrete	8.3E–10	Thomson et al. 2008b	8.3E–10
Concrete grout (backfill) in Silo (Porous concrete)	8.3e–09	Thomson et al. 2008b	3.0E–8
Concrete grout in BTF	8.3e–09	Thomson et al. 2008b	3.0E–9
Bentonite in Silo, upper part	9.0E–11	Thomson et al. 2008b	2.0E–10
Bentonite in Silo, lower part	9.0E–12	Thomson et al. 2008b	2.0E–12
10/90 Sand/Bentonite	1.0E–09	Thomson et al. 2008b	1.0E–9
Sand/gravel	High	Thomson et al. 2008b	High

B.2 Flow data

Table B-5. Water flow rate through repository parts at different times, m^3/year (Abarca et al. 2013)

Climate scenario	Tunnel	Tunnel Flow Rate (m^3/y)*	Waste Flow Rate (m^3/y)*
2000 AD	BMA	0.046	0.008
3000 AD	BMA	30.385	1.275
5000 AD	BMA	66.547	3.429
2000 AD	BLA	0.133	0.123
3000 AD	BLA	65.22	61.359
5000 AD	BLA	146.805	138.996
2000 AD	BTF1	0.028	0.009
3000 AD	BTF1	7.801	1.716
5000 AD	BTF1	17.947	3.498
2000 AD	BTF2	0.047	0.009
3000 AD	BTF2	19.891	2.424
5000 AD	BTF2	43.482	4.568
2000 AD	Silo	0.005	0.005
3000 AD	Silo	0.741	0.682
5000 AD	Silo	1.471	1.357

The values used in the calculations are done with preliminary values as of 2012 11 27. No important differences are observed between them.

B.3 Distribution coefficients (Kd)

Distribution coefficients (Kd) for concrete/cement for degradation state I, II and III. Non-saline conditions and absence of organic complexants are taken from the SR-PSU data report (SKB 2014a)

B.4 Radionuclide inventory data

Table B-9. Radionuclide inventory in SFR repository. Activity at year 2075 (SKB 2013)[3].

Nuclide	Silo [Bq]	BRT [Bq]	1BMA [Bq]	XBMA [Bq]	1BTF [Bq]	2BTF [Bq]	1BLA [Bq]	XBLA [Bq]	Total [Bq]
H-3	7.32E+09	0.00E+00	3.88E+08	3.16E+12	1.29E+08	6.19E+07	2.30E+08	1.55E+11	3.33E+12
Be-10	9.44E+05	0.00E+00	2.03E+05	2.10E+04	1.39E+04	2.75E+04	5.72E+02	1.29E+03	1.21E+06
C-14 org	6.31E+11	0.00E+00	1.39E+11	6.38E+09	1,05E+10	5,33E+09	8,17E+07	2,33E+08	7,93E+11
C-14 oorg	2.37E+12	0,00E+00	1,36E+12	2,96E+11	2,34E+11	2,11E+11	4,14E+09	9,44E+08	4,48E+12
C-14 ind	0,00E+00	9,77E+09	1,50E+07	1,32E+10	0,00E+00	0,00E+00	0,00E+00	1,97E+09	2,50E+10
Cl-36	1,18E+09	6,90E+06	3,36E+08	2,00E+08	3,14E+07	1,32E+07	2,19E+07	4,52E+07	1,83E+09
Ca-41	0,00E+00	0,00E+00	1,53E+07	1,48E+10	0,00E+00	0,00E+00	0,00E+00	4,22E+09	1,90E+10
Fe-55	2,67E+12	5,36E+09	1,06E+08	7,61E+10	1,98E+08	1,42E+06	3,86E+04	3,89E+07	2,75E+12
Co-60	1,07E+13	1,13E+11	5,10E+10	1,27E+12	3,88E+10	3,26E+09	1.05E+08	5.67E+09	1.21E+13
Ni-59	6.70E+12	1.55E+11	2.15E+12	8.13E+11	3.29E+10	4.17E+10	3.38E+09	1.03E+10	9.91E+12
Ni-63	5.29E+14	1.38E+13	1.50E+14	7.93E+13	2.18E+12	2.29E+12	2.46E+11	8.53E+11	7.78E+14
Se-79	1.03E+09	0.00E+00	2.11E+08	2.33E+07	1.16E+07	2.07E+07	3.88E+05	6.71E+06	1.30E+09
Sr-90	4.54E+12	2.04E+10	4.87E+11	4.19E+11	7.29E+10	4.43E+10	5.66E+08	2.66E+10	5.61E+12
Zr-93	3.58E+09	1.83E+08	4.08E+08	1.03E+09	2.91E+07	4.59E+07	1.84E+06	2.18E+07	5.30E+09
Nb-93m	5.45E+12	9.19E+11	3.01E+11	1.17E+13	2.48E+09	1.65E+09	4.23E+07	5.06E+10	1.84E+13
Nb-94	6.40E+10	7.66E+09	8.20E+09	8.39E+10	2.61E+08	4.57E+08	3.53E+07	6.18E+08	1.65E+11
Mo-93	7.17E+09	2.86E+09	1.10E+09	3.97E+09	5.92E+07	1.74E+08	6.33E+06	1.42E+08	1.55E+10
Tc-99	2.38E+11	4.30E+08	1.64E+10	9.14E+09	5.91E+09	7.14E+08	3.29E+07	4.00E+08	2.71E+11
Pd-107	5.57E+09	0.00E+00	1.02E+08	2.83E+10	2.92E+06	5.19E+06	9.70E+04	6.16E+10	9.55E+10
Ag-108m	1.49E+11	1.52E+09	1.85E+10	3.49E+10	1.61E+09	2.43E+09	2.13E+08	1.04E+09	2.09E+11
Cd-113m	1.27E+10	0.00E+00	6.45E+08	8.81E+09	1.08E+08	4.18E+07	1.28E+06	4.77E+09	2.71E+10
In-115	0.00E+00	0.00E+00	0.00E+00	3.10E+05	0.00E+00	0.00E+00	0.00E+00	0.00E+00	3.10E+05
Sn-126	2.44E+10	7.00E+05	2.54E+08	1.31E+11	1.46E+06	2.59E+06	4.85E+04	2.94E+11	4.50E+11
Sb-125	1.32E+11	6.27E+06	2.23E+06	1.31E+08	1.78E+07	1.69E+05	1.55E+03	9.07E+05	1.32E+11
I-129	8.69E+08	0.00E+00	1.44E+08	1.13E+07	1.26E+07	1.39E+07	4.46E+05	2.29E+06	1.05E+09
Cs-134	2.20E+11	0.00E+00	4.95E+04	1.93E+08	1.63E+05	5.97E+02	1.66E+00	3.00E+05	2.20E+11
Cs-135	4.28E+09	0.00E+00	8.49E+08	7.64E+07	7.10E+07	2.03E+07	3.20E+06	1.72E+08	5.47E+09
Cs-137	5.55E+13	0.00E+00	7.60E+12	2.11E+12	7.54E+11	6.57E+11	1.59E+10	5.15E+11	6.72E+13
Ba-133	4.97E+08	0.00E+00	1.92E+07	1.34E+08	8.07E+06	3.04E+06	8.52E+04	9.58E+06	6.71E+08
Pm-147	3.57E+11	5.89E+05	2.53E+06	4.36E+08	8.74E+06	3.64E+04	1.14E+03	3.67E+06	3.58E+11
Sm-151	4.44E+11	3.13E+08	8.22E+10	4.20E+10	5.51E+09	7.75E+09	1.58E+08	5.84E+09	5.88E+11
Eu-152	7.73E+08	4.28E+05	4.02E+09	1.22E+11	1.04E+08	4.12E+06	1.12E+08	1.44E+10	1.41E+11
Eu-154	4.46E+11	6.71E+07	9.50E+09	1.65E+10	3.39E+09	5.58E+08	1.83E+07	3.15E+08	4.76E+11
Eu-155	9.41E+10	1.41E+06	1.14E+08	8.07E+08	1.06E+08	4.08E+06	1.25E+05	1.16E+07	9.52E+10
Ho-166m	7.75E+09	7.44E+03	1.51E+09	6.77E+08	1.13E+08	1.75E+08	7.06E+06	9.29E+07	1.03E+10
U-232	6.11E+05	6.31E+03	1.56E+06	3.06E+05	6.78E+03	6.09E+03	5.15E+01	6.49E+03	2.50E+06
U-234	3.48E+07	0.00E+00	9.08E+07	7.43E+06	4.01E+05	4.60E+05	3.80E+03	3.25E+03	1.34E+08
U-235	1.36E+07	1.52E+01	8.20E+06	5.99E+05	3.89E+07	1.76E+05	5.28E+08	5.79E+08	1.17E+09
U-236	1.62E+07	3.65E+05	3.03E+07	9.65E+06	2.25E+05	4.15E+05	1.24E+03	2.47E+05	5.74E+07
U-238	3.18E+07	0.00E+00	6.79E+08	7.65E+07	5.78E+08	9.35E+05	2.34E+09	1.26E+08	3.84E+09
Np-237	5.31E+08	4.40E+05	6.41E+07	1.64E+07	7.60E+05	2.33E+06	2.43E+05	2.61E+05	6.15E+08
Pu-238	6.93E+10	2.49E+09	6.43E+10	3.91E+10	1.18E+09	4.33E+08	8.04E+07	6.58E+08	1.78E+11
Pu-239	1.82E+10	3.87E+08	4.08E+10	1.20E+10	7.04E+08	1.91E+08	5.26E+07	3.24E+08	7.26E+10
Pu-240	2.55E+10	5.55E+08	5.71E+10	1.38E+10	9.86E+08	2.67E+08	7.37E+07	4.51E+08	9.87E+10
Pu-241	2.56E+11	7.28E+09	5.81E+11	2.22E+11	3.38E+09	1.19E+09	1.08E+07	5.11E+08	1.07E+12
Pu-242	1.19E+08	2.89E+06	2.94E+08	6.07E+07	1.20E+06	1.38E+06	1.14E+04	2.04E+05	4.80E+08
Am-241	2.32E+13	1.95E+09	4.03E+11	6.34E+10	2.26E+09	1.86E+09	1.09E+10	4.62E+08	2.37E+13
Am-242m	3.10E+08	1.23E+07	7.21E+08	2.08E+08	3.02E+06	3.08E+06	2.58E+04	8.47E+05	1.26E+09
Am-243	1.50E+09	3.84E+07	2.94E+09	7.54E+08	1.46E+07	1.74E+07	1.06E+05	3.05E+06	5.27E+09
Cm-243	1.77E+08	5.65E+06	4.38E+08	1.31E+08	6.73E+05	3.87E+05	1.06E+04	4.45E+05	7.53E+08
Cm-244	8.59E+09	5.71E+08	1.02E+10	9.21E+09	1.88E+08	1.54E+07	1.21E+07	1.54E+08	2.90E+10
Cm-245	1.44E+07	6.40E+05	2.94E+07	1.11E+07	1.20E+05	1.37E+05	1.13E+03	4.81E+04	5.59E+07
Cm-246	4.18E+06	2.11E+05	7.83E+06	3.60E+06	3.18E+04	3.64E+04	3.01E+02	1.66E+04	1.59E+07
Total	**6.43E+14**	**1.51E+13**	**1.64E+14**	**1.00E+14**	**3.35E+12**	**3.27E+12**	**2.85E+11**	**2.01E+12**	**9.31E+14**

[3] Values taken from an earlier version of SKB 2013. In this report the values from the earlier version has been used. The conclusions drawn are judged not to be affected.

Table B-10. Half-lives recommended for use in SR-PSU (SKB 2014a).

Nuclide	Half-life [years]			Nuclide	Half-life [years]		
		Min.	Max.			Min.	Max.
Ag-108m[a)]	438	429	447	Ni-63	100.1	98.1	102.1
Am-241	432.2	431.5	432.9	Np-237	2.144E+06	2.137E+06	2.151E+06
Am-242m	141	139	143	Pd-107	6.5E+06	6.2E+06	6.8E+06
Am-243	7,370	7,330	7,410	Pm-147	2.6234	2.6232	2.6236
Ba-133	10.51	10.46	10.56	Pu-238	87.7	87.4	88.0
Be-10	1.51E+06	1.45E+06	1.57E+06	Pu-239	24,110	24,080	24,140
C-14inorg	5,730	5,690	5,770	Pu-240	6,563	6,556	6,570
Cd-133m	14.1	13.6	14.6	Pu-241	14.35	14.25	14.45
Cl-36	3.01E+05	2.99E+05	3.03E+05	Pu-242	3.733E+05	3.721E+05	3.745E+05
Cm-243	29.1	29.0	29.2	Ru-106	373.59 d	373.44 d	373.74 d
Cm-244	18.10	18.08	18.12	Sb-125	2.7582	2.7571	2.7593
Cm-245	8,500	8,400	8,600	Se-79[b)]	3.27E+05	3.19E+05	3.35E+05
Cm-246	4,730	4,630	4,830	Sm-151	90	82	98
Co-60	5.2714	5.2709	5.2719	Sn-126	~1E+05		
Cs-134	2.0648	2.0638	2.0658	Sr-90	28.78	28.74	28.82
Cs-135	2.3E+06	2.0E+06	2.6E+06	Tc-99	2.111E+05	2.099E+05	2.123E+05
Cs-137	30.07	30.04	30.10	U-232	68.9	68.5	69.3
Eu-152	13.537	13.531	13.543	U-234	2.455E+05	2.449E+05	2.461E+05
Eu-154	8.593	5.589	8.597	U-235	7.038E+08	7.033E+08	7.043E+08
Eu-155	4.7611	4.7598	4.7624	U-236	2.342E+07	2.339E+07	2.345E+07
Fe-55	2.73	2.70	2.76	U-238	4.468E+09	4.465E+09	4.471E+09
H-3	12.33	12.26	12.39	Zr-93	1.53E+06	1.43E+06	1.63E+06
Ho-166m	1.20E+03	1.02E+03	1.38E+03				
I-129	1.57E+07	1.53E+07	1.61E+07				
Mo-93	4.0E+03	3.2E+03	4.8E+03				
Nb-93m	16.13	15.99	16.27				
Nb-94	2.03E+04	1.87E+04	2.19E+04				
Ni-59	7.6E+04	7.1E+04	8.1E+04				

All data taken from Firestone et al. (1998) except for a) Schrader (2004) and b) Jörg et al. (2010).